

Linguistic Collapse: Neural Collapse in (Large) Language Models

Robert Wu
University of Toronto
rupert@cs.toronto.edu

Vardan Papyan
University of Toronto
vardan.papyan@utoronto.ca

Abstract

Neural collapse (\mathcal{NC}) is a phenomenon observed in classification tasks where top-layer representations collapse into their class means, which become equinorm, equiangular and aligned with the classifiers. These behaviors – associated with generalization and robustness – would manifest under specific conditions: models are trained towards zero loss, with noise-free labels belonging to balanced classes, which do not outnumber the model’s hidden dimension. Recent studies have explored \mathcal{NC} in the absence of one or more of these conditions to extend and capitalize on the associated benefits of ideal geometries. Language modeling presents a curious frontier, as *training by token prediction* constitutes a classification task where none of the conditions exist: the vocabulary is imbalanced and exceeds the embedding dimension; different tokens might correspond to similar contextual embeddings; and large language models (LLMs) in particular are typically only trained for a few epochs. This paper empirically investigates the impact of scaling the architectures and training of causal language models (CLMs) on their progression towards \mathcal{NC} . We find that \mathcal{NC} properties that develop with scaling are linked to generalization. Moreover, there is evidence of some relationship between \mathcal{NC} and generalization independent of scale. Our work therefore underscores the generality of \mathcal{NC} as it extends to the novel and more challenging setting of language modeling. Downstream, we seek to inspire further research on the phenomenon to deepen our understanding of LLMs – and neural networks at large – and improve existing architectures based on \mathcal{NC} -related properties.

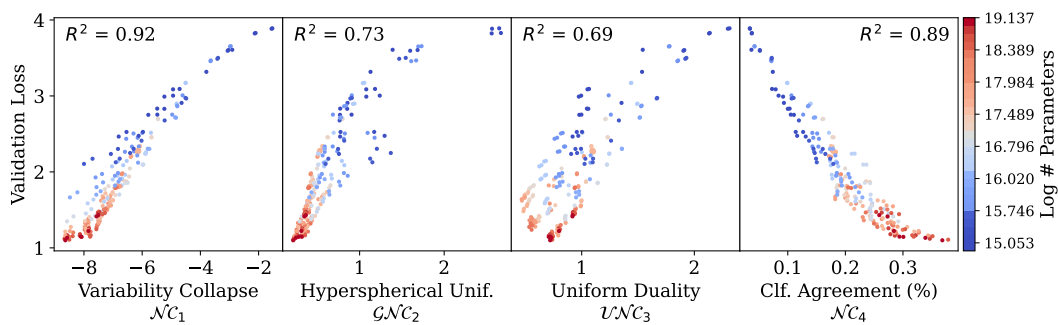


Figure 1: Simultaneous development of the four *neural collapse* (\mathcal{NC}) [1] properties in 230 causal language models trained on TinyStories [2], alongside improvement in generalization (i.e. validation performance). Left to right: \mathcal{NC}_1) within-class (representation) variability collapse; \mathcal{GNC}_2) hyper-spherical uniformity of class means; \mathcal{UNC}_3) uniform duality between class means and corresponding classifiers; and \mathcal{NC}_4) agreement between token (maximum a priori) classifiers and implicit nearest-class center classifiers. Colored by model size and annotated with coefficient of determination (R^2).

1 Introduction

1.1 Neural Collapse

A learning phenomenon known as *neural collapse* (\mathcal{NC}) emerges during the terminal phase of training neural networks with cross-entropy (CE) loss for classification [1]. It was originally characterized as the co-occurrence of the following properties in a model’s top-layer features (also known as last-layer representations or embeddings) and classifiers:

- (\mathcal{NC}_1) **Within-class variability collapse:** Top-layer features collapse to their class means.
- (\mathcal{NC}_2) **Convergence to a simplex ETF:** Class means tend towards equinorm and equiangular vectors when centered about the global average. The resulting geometry – known as a simplex *equiangular tight frame* (ETF) – maximizes pairwise angles and distances.
- (\mathcal{NC}_3) **Convergence to self-duality:** Top-layer classifier vectors converge to their corresponding class means, and thus also form a simplex ETF.
- (\mathcal{NC}_4) **Nearest decision rule:** Linear classifiers approximate a nearest-class center (NCC) classifier: top-layer embeddings predict the class with the closest mean (implied by \mathcal{NC}_1 -3).

These behaviors, often associated with improved generalization and robustness (among other benefits, such as those discussed in §1.4), traditionally manifest under the following conditions:

- C1) **Few classes:** The number of classes is upper-bounded by the embedding dimension plus one: $C \leq d + 1$; this is required to construct a perfect simplex ETF.
- C2) **Balanced classes:** The number of samples is equal across classes: $N_c = N_{c'}, \forall c \neq c'$.
- C3) **Noise-free labels:** Identical (or very similar) embeddings should belong to the same class.
- C4) **Terminal phase of training (TPT):** The model is trained past zero error, towards zero loss.

Absent these conditions, one does not typically anticipate \mathcal{NC} . Since then, follow-up studies have extended beyond and proposed techniques of quantifying or achieving \mathcal{NC} (discussed in Section 2).

1.2 (Large) Language Models

\mathcal{NC} is a phenomenon observed specifically in classification tasks. While not traditionally thought of as classifiers, language models – including large language models (LLMs) – learn to model aleatoric uncertainty, which can be viewed as stochastic token prediction [3]. For instance, masked language models (MLMs) such as BERT [4] predict one or several masked tokens within an input sequence based on the surrounding *context*. Likewise, autoregressive or causal language models (CLMs) such as GPT [5] predict the next token in a sequence given the *context* of previous tokens. Most of these models are essentially (*pre-*)trained by token classification on their vocabularies. This parallel – also drawn by [6] – raises a few natural questions:

1. Does the pre-training stage of a language model exhibit \mathcal{NC} ?
2. How do scaling and other training configurations influence \mathcal{NC} in (L)LMs?
3. To what extent is \mathcal{NC} in (L)LMs correlated with their generalization abilities?
4. Do such correlations, between \mathcal{NC} and improved generalization, persist independent of the (potential confounders of) model size and training?

To address these, we first examine the specific settings of training CLMs as they are opposed (\neg) to the prerequisites (C1-4, §1.1) for \mathcal{NC} to manifest.

- \neg C1) **Many classes:** The unique tokens found in language modeling vocabularies are vast, usually numbering in the tens of thousands and far exceeding the hidden dimension [7].
- \neg C2) **Imbalanced classes:** The distribution of tokens in natural language is typically very imbalanced [8, 9], as is the case in TinyStories [2], the dataset we use (Appendix Figure 4). It has an average of 16K samples per class but a standard deviation of over 32K.

- C3) **Ambiguous contexts:** There may exist very similar or even identical contexts followed by different tokens in the natural language data [10]. For instance, over half of the sequences in TinyStories [2] lead with “Once upon a time”, but only three-quarters of these follow with a comma (“Once upon a time,”). In other words, there is almost certainly some *ambiguity* to contend with in our context embeddings.
- C4) **Undertraining:** Most practical language models (including LLMs) are not trained for more than a few epochs [11, 12]. Further optimization typically renders diminishing returns in improving evaluation performance [13] long before any possible TPT.

1.3 Contributions

We train a suite of Transformer-based [14] CLMs¹ across a grid of model widths, depths, and training epochs on the TinyStories dataset [2] to assess the degrees to which \mathcal{NC} properties develop and how they relate to generalization performance. Our findings (summarized in Figure 1) reveal:

- **Emergence of \mathcal{NC} with scale:** As we scale model size and training, the properties of \mathcal{NC} emerge; within-class variability (\mathcal{NC}_1) and interference are reduced while hyperspherical uniformity (\mathcal{GNC}_2), uniform duality (\mathcal{UNC}_3), and classifier agreement (\mathcal{NC}_4) improve.
- **Progression towards hyperspherical uniformity:** Class means, while unable to form a simplex ETF (\mathcal{NC}_2), nonetheless tend towards uniform dispersion on a hypersphere, a geometry theorized by [15] and formalized by [16] as *hyperspherical uniformity* (\mathcal{GNC}_2).
- **Tendency towards uniform duality:** Direct alignment (self-duality) between class means and classifiers (\mathcal{NC}_3) does not appear to develop with scale. Instead, the variability of (mis)alignment across classes decreases with width and training, suggesting its minimization – which we term *uniform duality* (\mathcal{UNC}_3) – may be more cohesive with \mathcal{NC} .
- **Correlation between \mathcal{NC} and generalization:** The developments of \mathcal{NC} properties are correlated with improved validation performance. We show these correlations to persist even when fixing the (potential confounders of) model architecture and training by simply varying the random seeds for initialization and data shuffling. This suggests that \mathcal{NC} is not simply a side-effect of training, but possibly a factor of generalization in its own right.

1.4 Significance

Recently, methods building on \mathcal{NC} have found use in deep learning at large. We highlight areas such as federated learning [17], graph neural networks [18], incremental/continual learning [19–21], meta-learning [21, 22], out-of-distribution detection [23–25], privacy [26, 27], learning theory [28–33] transfer learning [34–39], and even LLM prompting [40]. With our results, we aim to extend insights from such contributions and other related works to the language modeling domain and ultimately assist researchers in improving and interpreting their (L)LMs.

2 Related Works

\mathcal{NC} was initially observed in image classification tasks such as on CIFAR-10/100 [41] and ImageNet [42]. Since then, the phenomenon has been further studied both theoretically and empirically [15, 32, 37, 43–65], with several works venturing into settings without some of the traditional prerequisites (C1-4, §1.1):

A large number of classes \mathcal{NC} established the simplex ETF as an optimal configuration. However, a perfect simplex ETF (\mathcal{NC}_2) requires that the number of classes C not exceed $d + 1$ where d is the embedding dimension. This requirement that d be sufficiently large is not practical when the classes number beyond the thousands. GPT-2 [66], for instance, has a vocabulary of over 50K tokens.²

In such a scenario, one might still expect class means to be uniformly distributed on a d -dimensional hypersphere [15]. [16] formalize this as *hyperspherical uniformity* within a *generalized neural collapse* (\mathcal{GNC}) framework, which [6] then empirically demonstrate. These latter two works mention

¹Our models range from 3.4M (small) to 205M (large), so we inclusively use “CLM” instead of “LLM”.

²Following [67], one might describe such a setting ($C > d + 1$) as a model “in superposition”.

language modeling as applicable for $\mathcal{GN}\mathcal{C}$; [6] even frame token prediction as a classification task, just as we do. We remark however that both earlier works *simulate* a large number of classes by drastically shrinking the embedding dimension. In contrast, we study next-token prediction, using the full class space (vocabulary) with an imbalanced token distribution and ambiguous samples.

Class imbalance \mathcal{NC} traditionally assumed that classes were sample-balanced. Since then, follow-up works have investigated the effect of class imbalance on the prevalence of \mathcal{NC} . [46] studied the *layer-peeled model* (LPM) and discovered that *minority collapse* occurs when classes are imbalanced across two equally-sized groups of classes; a threshold for minority collapse was later characterized by [32]. [51] showed that \mathcal{NC} still occurs in such an LPM when the classifier is initialized as a fixed ETF. [68] introduced *simplex-encoded-label interpolation* (SELI) but noted that more severe imbalance worsens even this geometry. Recently, feature regularization has been employed to induce \mathcal{NC} and improve generalization in class-imbalanced settings [57, 60, 61].

Multi-label classification In some problems, one might encounter mixed or multi-label samples, be they natural or due to noise or augmentation [69, 70]. \mathcal{NC} was also recently studied for such data by [63], who observed that multi-label class means arrive at the average of their individual labels’ means. They also devise an augmented CE loss function to accommodate such samples.

However, most of our ambiguous samples are not soft- nor multi-label, but rather identical (or very similar) context samples with different hard token labels ($\neg\mathcal{C}3$, §1.2). This effectively rules out the prospect of achieving zero classification error and potentially introduces irreducible noise.

A recent study showed that memorization of noisy labels likely leads to degradation of \mathcal{NC} [59].

Early stages of training [52] studied \mathcal{NC} in small ResNet [71] models that had not yet converged (similar to most LLMs). They show that within-class variability drops and “plateaus” ($\mathcal{NC}1$) earlier than other \mathcal{NC} metrics, a result that we also observe (§4.1, Figures 5, 14).

Natural language processing (NLP) An earlier study reported that the ratio of within-class to between-class covariances of word embeddings increases with model depth [72, 73], seemingly at odds with $\mathcal{NC}1$. It can however be distinguished from literature studying layer-wise \mathcal{NC} in that it does not center the mean representation vectors (i.e. subtract the global mean).

[16] fine-tuned BERT [4] using their *hyperspherical uniformity gap* (HUG) objective on binary classification tasks from the GLUE benchmark [74]. [75] conducted a tangentially-related investigation of convolutional neural networks for few-class semi-supervised clustering in which they identify \mathcal{NC} . Our work is distinct from these in several ways: a) our class space far exceeds our embedding dimension ($C \gg d + 1$) because we classify on the full token vocabulary; b) we analyze embeddings at a token-level granularity rather than at the sequence level; and c) our next token prediction is causal (context-dependent) as opposed to the per-sample independence of their few-category classification.

A more related work studied *feature collapse* in individual word representations [76], but the authors note that their analysis is limited to shallow NLP modeling on more rigid and symmetrical text data.

3 Methodology

In this section, we describe the training setup for our CLMs (§3.1), procedures for collecting top-layer embeddings (§3.2, 3.7), and measurements of \mathcal{NC} and generalization (§3.4, 3.5, 3.6, 3.7, 3.8).

3.1 Dataset and Language Models

TinyStories is a synthetic³ dataset generated by GPT-3.5 and GPT-4 [2] with token vocabulary $\mathbb{V} = \llbracket 1, 29233 \rrbracket$. Token prediction can therefore be framed as classification among $C = 29,233$ token classes.⁴ Following the GPT-style regime[5], raw sequences are packed into S chunks of size T , providing $N = S(T - 1)$ token samples for training.⁵ Details are listed in Appendix B.

³TinyStories was developed and evaluated as a faithful emulation of large language modeling [2], so we chose it for experimentation to train hundreds of CLMs and analyze embeddings at low cost. See Appendix B.

⁴Although the GPT-2 [77] tokenizer has over 50K tokens, only a subset vocabulary appears in TinyStories.

⁵We cannot use the first ground-truth nor last predicted token in any chunk.

We use 30 CLM architectures based on GPT Neo [78], configured similarly to [2]. They vary in width (embedding dimension) $d \in \{64, 128, 256, 512, 768, 1024\}$ and depth (number of self-attention layers) $L \in \{1, 2, 4, 8, 12\}$. Our models were trained by teacher-forcing⁶ using CE loss. For each architecture, we trained multiple models for 1, 3, and 10 epochs. We albatred over weight decay factors $\beta = 0.0005$ [50] and $\beta = 0.1$ [77]. Further details are listed in Appendices A, C.

3.2 Context Embeddings

Base CLMs perform next-token prediction: given a sequence of tokens $\mathbf{x}_{1:t} \in \mathbb{V}^t$, a top-layer context embedding $\mathbf{h}(\mathbf{x}_{1:t}) \in \mathbb{R}^d$ is used to predict the next token $x'_{t+1} \in \mathbb{V}$ where $1 \leq t \leq T$. A classifier for class c with weights \mathbf{w}_c and bias⁷ b_c would make maximum a prior (MAP) predictions as

$$x'_{t+1} := \operatorname{argmax}_{c \in \mathbb{V}} \langle \mathbf{w}_c, \mathbf{h}(\mathbf{x}_{1:t}) \rangle + b_c. \quad (1)$$

Class embedding means For each token class c , we are interested in the mean embedding $\boldsymbol{\mu}_c \in \mathbb{R}^d$ across sequences s and their contexts $\mathbf{x}_{1:t}^{(s)}$, where the next token $x_{t+1}^{(s)}$ is ground-truth ($t < T$) and equal to c . To center these means, we compute their unweighted⁸ average $\bar{\boldsymbol{\mu}} \in \mathbb{R}^d$. Precisely, we take

$$\boldsymbol{\mu}_c := \frac{1}{N_c} \sum_{s=1}^S \sum_{t=1}^{T-1} \mathbf{h}(\mathbf{x}_{1:t}^{(s)}) \mathbb{I}(x_{t+1}^{(s)} = c), \quad \bar{\boldsymbol{\mu}} := \frac{1}{C} \sum_{c=1}^C \boldsymbol{\mu}_c, \quad (2)$$

where N_c is the number of samples of class c and \mathbb{I} is the (binary) indicator function.

Class embedding variances In a second pass, we accumulate the unbiased sample variances⁹:

$$\sigma_c^2 := \frac{1}{N_c - 1} \sum_{s=1}^S \sum_{t=1}^{T-1} \left\| \mathbf{h}(\mathbf{x}_{1:t}^{(s)}) - \boldsymbol{\mu}_c \right\|_2^2 \mathbb{I}(x_{t+1}^{(s)} = c). \quad (3)$$

3.3 Homogeneity and Variability

For some collapse measures (such as $(\mathcal{G})\mathcal{NC}_2$ and \mathcal{NC}_3), we are primarily interested in the *variation* rather than the average of pair-wise relationships. To that end, we also include in our analysis the *coefficient of variation* (CoV) of several measurements, which is the ratio of their standard deviations to their means: $\sigma(\cdot)/\mu(\cdot)$. We can interpret this as a normalized measure of variability.

3.4 Signal-to-Noise Ratio – \mathcal{NC}_1

The ability to disambiguate between classes depends on the ratio of within-class to between-class variabilities. Building upon foundational works [82, 83], \mathcal{NC} originally measured variability through an inverse *signal-to-noise ratio* (SNR), whose minimization constitutes *within-class variability collapse* (\mathcal{NC}_1). We employ the *class-distance normalized variance* (CDNV) proposed by [34]:

$$\text{CDNV}_{c,c'} := \frac{\sigma_c^2 + \sigma_{c'}^2}{2\|\boldsymbol{\mu}_c - \boldsymbol{\mu}_{c'}\|_2^2}, \quad \forall c \neq c'. \quad (4)$$

These pair-wise measures constitute the off-diagonal¹⁰ entries of a symmetric matrix in $\mathbb{R}^{C \times C}$, whose average we use as an inverse SNR. Within-class variability collapse is then re-characterized by the minimization of this quantity: $\text{CDNV}_{c,c'} \rightarrow 0, \forall c \neq c'$. This alternative convergence is faithful to \mathcal{NC}_1 but more robust and numerically stable [34].

3.5 Geometric Structures – $(\mathcal{G})\mathcal{NC}_2$

The separability of our representations also depends on the geometric structures found in our embeddings. [1] characterize \mathcal{NC}_2 as convergence to a *simplex equiangular tight frame* (ETF) [84, 85].

⁶Parallelized training using sequences' ground-truth labels for context as opposed to predicted tokens.

⁷Similar to many CLMs [78–81], our classifiers do not include additive biases, so $b_c = 0$.

⁸Different from most literature where classes were balanced and weighting is already equal.

⁹This sample variance is computed across all unnormalized dimensional entries.

¹⁰The main diagonal of CDNVs is undefined (due to the zero denominator) and ignored.

Equinormness Such a near-orthonormal configuration firstly implies that class means are equinorm:

$$\log \|\boldsymbol{\mu}_c - \bar{\boldsymbol{\mu}}\|_2 - \log \|\boldsymbol{\mu}_{c'} - \bar{\boldsymbol{\mu}}\|_2 \rightarrow 0, \quad \forall c \neq c'. \quad (5)$$

We measure CoV in the *logarithms* of class mean norms to assess “equinormness”.

Equiangularity \mathcal{NC}_2 also entails that class means are equiangular about their center $\bar{\boldsymbol{\mu}}$: pair-wise distances and angles between their class means should be maximized and similar. Following [1], we measure *interference* (sometimes known as similarity or *coherence* [86, 87]). Its minimization,

$$\left\langle \frac{\boldsymbol{\mu}_c - \bar{\boldsymbol{\mu}}}{\|\boldsymbol{\mu}_c - \bar{\boldsymbol{\mu}}\|_2}, \frac{\boldsymbol{\mu}_{c'} - \bar{\boldsymbol{\mu}}}{\|\boldsymbol{\mu}_{c'} - \bar{\boldsymbol{\mu}}\|_2} \right\rangle \rightarrow \frac{-1}{C-1}, \quad \forall c \neq c', \quad (6)$$

together with equinormness (Equation 5) constitute convergence to a simplex ETF. Although this geometry is not ultimately attainable since there are too many classes ($C > d + 1$), it can still be meaningful to measure a model’s tendency towards one. As with CDNV noise (Equation 4), pair-wise interferences form off-diagonal¹¹ entries in a symmetric matrix in $\mathbb{R}^{C \times C}$. The minimization of CoV in interferences therefore expresses the degree of “equiangularity”.

Hyperspherical uniformity A relaxation from the ETF is *hyperspherical uniformity* (\mathcal{GNC}_2), with mean vectors $\boldsymbol{\mu}_c$ uniformly distributed on the d -dimensional hypersphere [15, 16]. We gauge the degree of this uniformity with pair-wise interactions under a logarithmic inverse distance kernel:¹²

$$\log \left\| \frac{\boldsymbol{\mu}_c - \bar{\boldsymbol{\mu}}}{\|\boldsymbol{\mu}_c - \bar{\boldsymbol{\mu}}\|_2} - \frac{\boldsymbol{\mu}_{c'} - \bar{\boldsymbol{\mu}}}{\|\boldsymbol{\mu}_{c'} - \bar{\boldsymbol{\mu}}\|_2} \right\|^{-1}, \quad \forall c \neq c'. \quad (7)$$

3.6 Alignment Between Classifiers and Class Mean Embeddings – $(\mathcal{U})\mathcal{NC}_3$

The linear classifiers $\{\boldsymbol{w}_c\}_{c=1}^C$ lie in a dual vector space to that of the class means $\{\boldsymbol{\mu}_c\}_{c=1}^C$. While convergence to self-duality (\mathcal{NC}_3) was previously measured as distances [1] between class means classifiers (Equation 11), we instead simplify (\mathcal{NC}_3) as class-wise similarities:

$$\left\langle \frac{\boldsymbol{w}_c}{\|\boldsymbol{w}_c\|_2}, \frac{\boldsymbol{\mu}_{c'} - \bar{\boldsymbol{\mu}}}{\|\boldsymbol{\mu}_{c'} - \bar{\boldsymbol{\mu}}\|_2} \right\rangle \rightarrow 1, \quad \forall c \in \mathbb{V}. \quad (8)$$

We define *uniform duality* (\mathcal{UNC}_3) to be the minimization of the CoV of these similarities.

3.7 Agreement of the Classifiers – \mathcal{NC}_4

Finally, \mathcal{NC}_4 is described as the simplification of the linear classifier’s MAP predictions (Equation 1) for *test*¹³ points to those of the implicit *nearest-class center* (NCC) classifier:

$$\operatorname{argmax}_{c \in \mathbb{V}} \langle \boldsymbol{w}_c, \boldsymbol{h} \rangle + b_c \rightarrow \operatorname{argmin}_{c \in \mathbb{V}} \|\boldsymbol{h} - \boldsymbol{\mu}_c\|_2. \quad (9)$$

We calculate¹⁴ agreement as the proportion of samples on which the classifiers agree:¹⁵

$$\frac{1}{N_{\text{val}}} \sum_{s=1}^{S_{\text{val}}} \sum_{t=1}^{T_{\text{val}}-1} \mathbb{I} \left(x'_{t+1}^{(s)} = \operatorname{argmin}_{c \in \mathbb{V}} \left\| \boldsymbol{h} \left(x_{1:t}^{(s)} \right) - \boldsymbol{\mu}_c \right\|_2 \right). \quad (10)$$

3.8 Probing a Relationship Between \mathcal{NC} and Generalization

To isolate the effect of \mathcal{NC} on generalization independent of model scaling and training (if it exists), we selected a two-layer 768-wide architecture of which to train twenty more instances with weight decay $\beta = 0.0005$, each with a different data shuffling seed. We then followed the remainder of the pipeline described above to collect and analyze embeddings with respect to \mathcal{NC} . Finally, we performed a permutation test with 10^4 trials to determine the statistical significance of any correlation between \mathcal{NC} and generalization that remains when we hold constant all factors but shuffling seeds.

¹¹The main diagonal of interferences is equal to $\mathbf{1}$ (maximal coherence or self-similarity).

¹²Following [16], we employ the logarithmic inverse distance kernel $K_{\log}(\boldsymbol{a}, \boldsymbol{b}) = \log \|\boldsymbol{a} - \boldsymbol{b}\|^{-1}$ for its ability to emphasize gaps between small distances while scaling down the effect of larger distances.

¹³We used the validation set since it was not used for training or hyperparameter optimization.

¹⁴In practice, we use an equivalent decomposition (Eq. 12).

¹⁵Note that agreement is not equivalent to accuracy.

4 Results

In this section, we present the results from our empirical study on scaling and generalization:

- (\mathcal{NC}_1) Within-class variability is reduced across model scale (more so by width than depth) and training (up to 6 epochs), and is tightly correlated with validation performance.
- (\mathcal{NC}_2) Equinormness/equiangularity shows some improvement with scale, training, and performance. Hyperspherical uniformity ($\mathcal{GN}\mathcal{C}_2$) also improves but more clearly and consistently.
- (\mathcal{NC}_3) Our models fail to achieve self-duality: class means do not align with classifiers. However, uniform duality ($\mathcal{UN}\mathcal{C}_3$) is correlated with model width, training, and performance.
- (\mathcal{NC}_4) Larger or more trained models exhibit closer agreement between their linear and implicit NCC classifiers. Agreement is also associated with validation performance.

We find that \mathcal{NC} is generally promoted by model size and training and correlated with generalization (validation performance). We also discern some of this correlation independent of scale (§4.5).

4.1 Within-Class Variability Collapse – \mathcal{NC}_1

Scaling our models dramatically reduces normalized variance, which is further aided by more training epochs and stronger weight decay (Appendix Figs. 5, 6). These noise reductions tightly associate with generalization (Fig. 1, left, “ \mathcal{NC}_1 ”). The relationship is strongest at larger model scale.

4.2 Geometric Structures – (\mathcal{G}) \mathcal{NC}_2

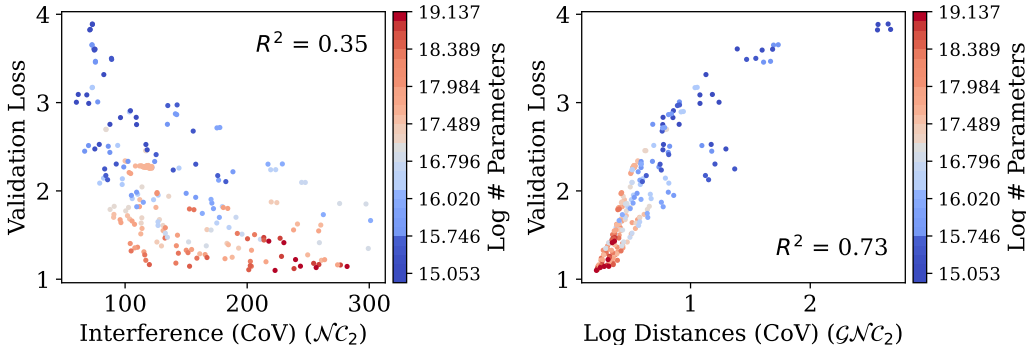


Figure 2: Validation loss shows a negligible correlation with equiangularity (\mathcal{NC}_2 , left) but a strong one with hyperspherical uniformity ($\mathcal{GN}\mathcal{C}_2$, right). In other words, $\mathcal{GN}\mathcal{C}_2$ develops with scale and correlates well with generalization, much better than \mathcal{NC}_2 .

Equinormness Mean norms grow with model width and training (Appendix Fig. 7), and subtly with depth (Appendix Fig. 8). Despite this growth, the variation of norms consistently decreases with scale (Appendix Figs. 9, 10). Both trends correlate with improved generalization (Appendix Fig. 25).

Equiangularity Scaling model dimensions reduces average interference (Appendix Figs. 11, 12) down to an empirical plateau of approximately 10^{-3} , which is more apparent in less-trained models. However, the variation of interference rises and persists when scaling (Appendix Figs. 13, 14), suggesting that interference becomes more concentrated between some pairs of classes. These results could be due to various factors, including but not limited to unfriendly conditions of language modeling (§1.2) or the impossibility of a simplex ETF (§3.5).

We only see a rough correlation between average interference and generalization and almost none with its variation, equiangularity (Appendix Fig. 26). In other words, the limited trends we observed toward a simplex ETF do not appear to be associated with generalization when $C > d + 1$.

Hyperspherical uniformity Logarithmic distances drop more gradually and consistently with scale (Appendix Figs. 15, 16), implying this quantity is more robust or may not face the same geometric barriers seen in conventional interference (Appendix Figs. 13, 14). Variation of these logarithmic distances is also consistently reduced with scale (Appendix Fig. 17, 18).

And finally, generalization has much stronger correlations with logarithmic distances than it has with regular interference (Fig. 2), validating the applicability of $\mathcal{GN}\mathcal{C}$ [16] when $C > d + 1$.

4.3 Classifier (Mis)alignment and Duality – $(\mathcal{U})\mathcal{N}\mathcal{C}_3$

Model width (d) is correlated faintly with average similarity between class means and their respective classifiers (Appendix Fig. 19), but strongly with variation in similarity (Appendix Fig. 21). The relationships to generalization follow the same pattern (Fig. 3), suggesting that uniform duality ($\mathcal{U}\mathcal{N}\mathcal{C}_3$) might serve as a better $\mathcal{N}\mathcal{C}$ property than self-duality ($\mathcal{N}\mathcal{C}_3$) overall; we discuss this in §4.5.

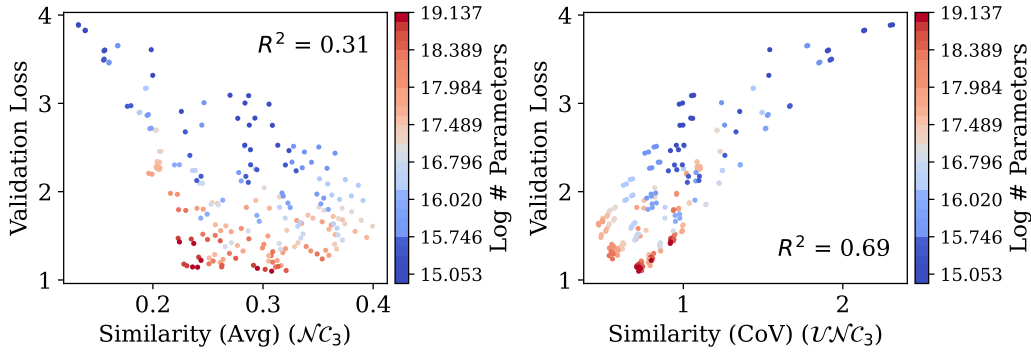


Figure 3: Validation loss shows a negligible relationship with self-duality ($\mathcal{N}\mathcal{C}_3$, left) and some correlation with uniform duality ($\mathcal{U}\mathcal{N}\mathcal{C}_3$, right). In other words, $\mathcal{U}\mathcal{N}\mathcal{C}_3$ develops with scale and correlates with generalization well and much better than $\mathcal{N}\mathcal{C}_3$.

4.4 Classifier Agreement – $\mathcal{N}\mathcal{C}_4$

The linear and NCC classifiers agree on far more examples than random chance. Scaling encourages agreement (Appendix Figs. 23, 24). Increasing width for certain depths happens to plateau or even regress the agreement rate, but this limitation is overcome with further training. And finally, agreement is a strong indicator of generalization (Fig. 1, right, $\mathcal{N}\mathcal{C}_4$).

4.5 Neural Collapse’s Relationship with Generalization

Table 1 presents the correlation scores of $\mathcal{N}\mathcal{C}$ metrics with generalization alongside their associated p-values from the permutation tests described in §3.8. The majority of the correlations are statistically significant ($p < 0.05$) independent of scale, affirming that $\mathcal{N}\mathcal{C}$ is correlated with generalization.

4.6 Duality of Duality

The dichotomy of self-duality ($\mathcal{N}\mathcal{C}_3$) and uniform duality ($\mathcal{U}\mathcal{N}\mathcal{C}_3$) is rather conspicuous. Our main experiments find that $\mathcal{N}\mathcal{C}_3$ does not consistently develop with scale while $\mathcal{U}\mathcal{N}\mathcal{C}_3$ does (Fig. 3). However, within fixed scale, the opposite is true, implying that $\mathcal{U}\mathcal{N}\mathcal{C}_3$ may be confounded by model capacity while $\mathcal{N}\mathcal{C}_3$ is a subtle and fine-grained indicator of generalization.

4.7 The Effect of Weight Regularization

Our models trained with either weight decay factor exhibited very similar patterns in the emergence of $\mathcal{N}\mathcal{C}$ (or lack thereof), but the more aggressive factor $\beta = 0.1$ typically used to train LLMs [77] resulted in stronger development of $\mathcal{N}\mathcal{C}$ properties (Appendices D, E, F, G, H, I, J, K, L, M).

Table 1: Permutation test of \mathcal{NC} measurements with respect to validation loss. Twenty-one (21) identical two-layer 768-wide models were trained with different data shuffling seeds and permuted with 10^4 trials. The p -values below 0.05 (bolded) show those properties to be statistically significant.

Property	Measurement	R^2 Correlation (\uparrow)	p -value (\downarrow)
$\mathcal{NC}1$	Within-Class Variability Collapse	0.192011	0.0485
$\mathcal{NC}2$	Equinormness	0.026174	0.4870
$\mathcal{NC}2$	Equiangularity	0.218574	0.0317
$\mathcal{GNC}2$	Hyperspherical Uniformity	0.487935	0.0002
$\mathcal{NC}3$	Self-Duality	0.322210	0.0063
$\mathcal{UNC}3$	Uniform Duality	0.000036	0.9784
$\mathcal{NC}4$	Classifier Agreement	0.490278	0.0001

5 Limitations

While to the best of our knowledge, no previous work has studied realistic stochastic token prediction, it is possible that the quantities that we measure are not perfectly suited for \mathcal{NC} in language modeling.

Our work is on causal language modeling in its most basic form. We did not conduct experiments into encoding, multi-modal, or instruction-tuned models.

The models that we used in our permutation test (§4.5, Table 1) are only of single small architecture. Therefore, our results on scale-independent \mathcal{NC} do not necessarily translate to larger models.

6 Discussion

Deep neural collapse (\mathcal{DNC}) A large body of work has established that properties resembling \mathcal{NC} evolve as a function of model depth [33, 52, 58, 59, 88–101]. Our results mostly concur, but encourage further exploration of \mathcal{DNC} in language modeling.

Learning to collapse Given the evidence for the development of \mathcal{NC} and associated generalization under various loss functions [16, 48, 59, 97, 102–104] in other domains, NLP researchers may also benefit from analyzing, adapting or training towards \mathcal{NC} with respect to alternative objectives.

Compression CLMs appear to reduce noise, demonstrating their ability to encapsulate different textual contexts into single embeddings. This subscribes to a theory that LLMs are essentially a compression of internet content by aleatoric modeling [105]. However, owing to contextual ambiguity, we hypothesize that CE loss and noise (Equation 4) cannot be fully eliminated by current practices.

Interpretability Our formulae (Section 3) and results (Section 4) expose the pair-wise token class interactions in noise, interference, classifier duality, and classifier agreement in the top-level features. Similarly to works in other domains [18, 54, 70, 106], these \mathcal{NC} metrics can serve as a form of low-level interpretability to aid understanding certain behaviors of (L)LMs.

Fairness Foundation models are ubiquitous for their comprehensive capabilities and adaptability. As previous work discussed class imbalance [32, 57, 60, 61], our work may extend these strategies to measure and perhaps promote fairness in foundation LLMs, some of which are designed to be multi-lingual or multicultural. While \mathcal{NC} itself would not lead to unfairness, its potential interpretability may, in theory, enable an adversarial agent to measure (un)fairness as they manipulate a LLM.

7 Conclusion

In this paper, we adapt the *neural collapse* (\mathcal{NC}) framework to the language modeling domain, where models are undertrained and next-tokens are variably drawn from numerous and imbalanced token classes. We leverage the canonical and more recent metrics to demonstrate that \mathcal{NC} emerges as we scale the size and training of hundreds of causal language models. Our results show a correlation between \mathcal{NC} and generalization, a relationship that persists even when the model scale is fixed.

With these novel insights, we hope to inspire new efforts to study \mathcal{NC} (and related behaviors) in language modeling and capitalize on their previously established benefits to improve and better understand the increasingly complex (large) language models and their training processes.

References

- [1] Vardan Papyan, X. Y. Han, and David L. Donoho. Prevalence of neural collapse during the terminal phase of deep learning training. *Proceedings of the National Academy of Sciences*, 117(40):24652–24663, sep 2020.
- [2] Ronen Eldan and Yuanzhi Li. Tinstories: How small can language models be and still speak coherent english?, 2023.
- [3] Emily M. Bender, Timnit Gebru, Angelina McMillan-Major, and Shmargaret Shmitchell. On the dangers of stochastic parrots: Can language models be too big? In *Proceedings of the 2021 ACM Conference on Fairness, Accountability, and Transparency*, FAccT ’21, page 610–623, New York, NY, USA, 2021. Association for Computing Machinery.
- [4] Jacob Devlin, Ming-Wei Chang, Kenton Lee, and Kristina Toutanova. Bert: Pre-training of deep bidirectional transformers for language understanding, 2019.
- [5] Alec Radford, Karthik Narasimhan, Tim Salimans, Ilya Sutskever, et al. Improving language understanding by generative pre-training. 2018.
- [6] Jiachen Jiang, Jinxin Zhou, Peng Wang, Qing Qu, Dustin Mixon, Chong You, and Zhihui Zhu. Generalized neural collapse for a large number of classes, 2023.
- [7] Zhilin Yang, Zihang Dai, Ruslan Salakhutdinov, and William W. Cohen. Breaking the softmax bottleneck: A high-rank rnn language model, 2018.
- [8] Claude Elwood Shannon. A mathematical theory of communication. *The Bell system technical journal*, 27(3):379–423, 1948.
- [9] P Sargant Florence. Human behaviour and the principle of least effort. *The Economic Journal*, 60(240):808–810, 1950.
- [10] Daniel Jurafsky and James H Martin. *Speech and language processing: An introduction to natural language processing, computational linguistics, and speech recognition*, 2009.
- [11] Jared Kaplan, Sam McCandlish, Tom Henighan, Tom B. Brown, Benjamin Chess, Rewon Child, Scott Gray, Alec Radford, Jeffrey Wu, and Dario Amodei. Scaling laws for neural language models, 2020.
- [12] Jordan Hoffmann, Sebastian Borgeaud, Arthur Mensch, Elena Buchatskaya, Trevor Cai, Eliza Rutherford, Diego de Las Casas, Lisa Anne Hendricks, Johannes Welbl, Aidan Clark, Tom Hennigan, Eric Noland, Katie Millican, George van den Driessche, Bogdan Damoc, Aurelia Guy, Simon Osindero, Karen Simonyan, Erich Elsen, Jack W. Rae, Oriol Vinyals, and Laurent Sifre. Training compute-optimal large language models, 2022.
- [13] Niklas Muennighoff, Alexander M. Rush, Boaz Barak, Teven Le Scao, Aleksandra Piktus, Nouamane Tazi, Sampo Pyysalo, Thomas Wolf, and Colin Raffel. Scaling data-constrained language models, 2023.
- [14] Ashish Vaswani, Noam Shazeer, Niki Parmar, Jakob Uszkoreit, Llion Jones, Aidan N Gomez, Lukasz Kaiser, and Illia Polosukhin. Attention is all you need. *Advances in neural information processing systems*, 30, 2017.
- [15] Jianfeng Lu and Stefan Steinerberger. Neural collapse with cross-entropy loss, 2021.
- [16] Weiyang Liu, Longhui Yu, Adrian Weller, and Bernhard Schölkopf. Generalizing and decoupling neural collapse via hyperspherical uniformity gap, 2023.

- [17] Zexi Li, Xinyi Shang, Rui He, Tao Lin, and Chao Wu. No fear of classifier biases: Neural collapse inspired federated learning with synthetic and fixed classifier. In *Proceedings of the IEEE/CVF International Conference on Computer Vision*, pages 5319–5329, 2023.
- [18] Vignesh Kothapalli, Tom Tirer, and Joan Bruna. A neural collapse perspective on feature evolution in graph neural networks. *Advances in Neural Information Processing Systems*, 36, 2024.
- [19] Yibo Yang, Haobo Yuan, Xiangtai Li, Jianlong Wu, Lefei Zhang, Zhouchen Lin, Philip Torr, Dacheng Tao, and Bernard Ghanem. Neural collapse terminus: A unified solution for class incremental learning and its variants, 2023.
- [20] Qin hao Zhou, Xiang Xiang, and Jing Ma. Hierarchical task-incremental learning with feature-space initialization inspired by neural collapse. *Neural Processing Letters*, 55(8):10811–10827, 2023.
- [21] Hang Ran, Weijun Li, Lusi Li, Songsong Tian, Xin Ning, and Prayag Tiwari. Learning optimal inter-class margin adaptively for few-shot class-incremental learning via neural collapse-based meta-learning. *Information Processing & Management*, 61(3):103664, 2024.
- [22] Saaketh Medepalli and Naren Doraiswamy. On the role of neural collapse in meta learning models for few-shot learning, 2023.
- [23] Jarrod Haas, William Yolland, and Bernhard Rabus. Linking neural collapse and l2 normalization with improved out-of-distribution detection in deep neural networks, 2023.
- [24] Mouin Ben Ammar, Nacim Belkhir, Sebastian Popescu, Antoine Manzanera, and Gianni Franchi. Neco: Neural collapse based out-of-distribution detection, 2024.
- [25] Jiawei Zhang, Yufan Chen, Cheng Jin, Lei Zhu, and Yuantao Gu. Epa: Neural collapse inspired robust out-of-distribution detector, 2024.
- [26] Donghao Li, Yang Cao, and Yuan Yao. Neuromixgdp: A neural collapse-inspired random mixup for private data release. In *Conference on Parsimony and Learning*, pages 480–514. PMLR, 2024.
- [27] Chendi Wang, Yuqing Zhu, Weijie J Su, and Yu-Xiang Wang. Neural collapse meets differential privacy: Curious behaviors of noisysGD with near-perfect representation learning, 2024.
- [28] Tolga Ergen, Arda Sahiner, Batu Ozturkler, John Pauly, Morteza Mardani, and Mert Pilanci. Demystifying batch normalization in relu networks: Equivalent convex optimization models and implicit regularization, 2022.
- [29] Tolga Ergen and Mert Pilanci. Revealing the structure of deep neural networks via convex duality. In Marina Meila and Tong Zhang, editors, *Proceedings of the 38th International Conference on Machine Learning*, volume 139 of *Proceedings of Machine Learning Research*, pages 3004–3014. PMLR, 18–24 Jul 2021.
- [30] Mariia Seleznova, Dana Weitzner, Raja Giryes, Gitta Kutyniok, and Hung-Hsu Chou. Neural (tangent kernel) collapse. In A. Oh, T. Naumann, A. Globerson, K. Saenko, M. Hardt, and S. Levine, editors, *Advances in Neural Information Processing Systems*, volume 36, pages 16240–16270. Curran Associates, Inc., 2023.
- [31] Matus Telgarsky. Feature selection with gradient descent on two-layer networks in low-rotation regimes, 2022.
- [32] Wanli Hong and Shuyang Ling. Neural collapse for unconstrained feature model under cross-entropy loss with imbalanced data, 2023.
- [33] Gerard Ben Arous, Reza Gheissari, Jiaoyang Huang, and Aukosh Jagannath. High-dimensional sgd aligns with emerging outlier eigenspaces, 2023.
- [34] Tomer Galanti, András György, and Marcus Hutter. On the role of neural collapse in transfer learning, 2022.

- [35] Like Hui, Mikhail Belkin, and Preetum Nakkiran. Limitations of neural collapse for understanding generalization in deep learning, 2022.
- [36] Tomer Galanti, András György, and Marcus Hutter. Improved generalization bounds for transfer learning via neural collapse. In *First Workshop on Pre-training: Perspectives, Pitfalls, and Paths Forward at ICML 2022*, 2022.
- [37] Vignesh Kothapalli. Neural collapse: A review on modelling principles and generalization. *Transactions on Machine Learning Research*, 2023.
- [38] Zijian Wang, Yadan Luo, Liang Zheng, Zi Huang, and Mahsa Baktashmotlagh. How far pre-trained models are from neural collapse on the target dataset informs their transferability. In *Proceedings of the IEEE/CVF International Conference on Computer Vision*, pages 5549–5558, 2023.
- [39] Anonymous. Understanding and improving transfer learning of deep models via neural collapse. *Submitted to Transactions on Machine Learning Research*, 2024. Under review.
- [40] Didi Zhu, Zexi Li, Min Zhang, Junkun Yuan, Yunfeng Shao, Jiashuo Liu, Kun Kuang, Yinchuan Li, and Chao Wu. Understanding prompt tuning for v-l models through the lens of neural collapse, 2023.
- [41] Alex Krizhevsky and Geoffrey Hinton. Learning multiple layers of features from tiny images. Technical Report 0, University of Toronto, Toronto, Ontario, 2009.
- [42] Jia Deng, Wei Dong, Richard Socher, Li-Jia Li, Kai Li, and Li Fei-Fei. Imagenet: A large-scale hierarchical image database. In *2009 IEEE conference on computer vision and pattern recognition*, pages 248–255. Ieee, 2009.
- [43] Dustin G. Mixon, Hans Parshall, and Jianzong Pi. Neural collapse with unconstrained features, 2020.
- [44] Tomaso Poggio and Qianli Liao. Explicit regularization and implicit bias in deep network classifiers trained with the square loss, 2020.
- [45] Weinan E and Stephan Wojtowytsch. On the emergence of simplex symmetry in the final and penultimate layers of neural network classifiers, 2021.
- [46] Cong Fang, Hangfeng He, Qi Long, and Weijie J Su. Exploring deep neural networks via layer-peeled model: Minority collapse in imbalanced training. *Proceedings of the National Academy of Sciences*, 118(43):e2103091118, 2021.
- [47] Zhihui Zhu, Tianyu Ding, Jinxin Zhou, Xiao Li, Chong You, Jeremias Sulam, and Qing Qu. A geometric analysis of neural collapse with unconstrained features, 2021.
- [48] X.Y. Han, Vardan Papyan, and David L. Donoho. Neural collapse under MSE loss: Proximity to and dynamics on the central path. In *International Conference on Learning Representations*, 2022.
- [49] Can Yaras, Peng Wang, Zhihui Zhu, Laura Balzano, and Qing Qu. Neural collapse with normalized features: A geometric analysis over the riemannian manifold. *Advances in neural information processing systems*, 35:11547–11560, 2022.
- [50] Akshay Rangamani and Andrzej Banburski-Fahey. Neural collapse in deep homogeneous classifiers and the role of weight decay. In *ICASSP 2022 - 2022 IEEE International Conference on Acoustics, Speech and Signal Processing (ICASSP)*, pages 4243–4247, 2022.
- [51] Yibo Yang, Shixiang Chen, Xiangtai Li, Liang Xie, Zhouchen Lin, and Dacheng Tao. Inducing neural collapse in imbalanced learning: Do we really need a learnable classifier at the end of deep neural network?, 2022.
- [52] Tom Tirer and Joan Bruna. Extended unconstrained features model for exploring deep neural collapse. In Kamalika Chaudhuri, Stefanie Jegelka, Le Song, Csaba Szepesvari, Gang Niu, and Sivan Sabato, editors, *Proceedings of the 39th International Conference on Machine Learning*, volume 162 of *Proceedings of Machine Learning Research*, pages 21478–21505. PMLR, 17–23 Jul 2022.

- [53] Peng Wang, Huikang Liu, Can Yaras, Laura Balzano, and Qing Qu. Linear convergence analysis of neural collapse with unconstrained features. In *OPT 2022: Optimization for Machine Learning (NeurIPS 2022 Workshop)*, 2022.
- [54] Jinxin Zhou, Chong You, Xiao Li, Kangning Liu, Sheng Liu, Qing Qu, and Zhihui Zhu. Are all losses created equal: A neural collapse perspective, 2022.
- [55] Akshay Rangamani, Marius Lindegaard, Tomer Galanti, and Tomaso A Poggio. Feature learning in deep classifiers through intermediate neural collapse. In *International Conference on Machine Learning*, pages 28729–28745. PMLR, 2023.
- [56] Tom Tirer, Haoxiang Huang, and Jonathan Niles-Weed. Perturbation analysis of neural collapse. In *International Conference on Machine Learning*, pages 34301–34329. PMLR, 2023.
- [57] Hien Dang, Tho Tran, Stanley Osher, Hung Tran-The, Nhat Ho, and Tan Nguyen. Neural collapse in deep linear networks: From balanced to imbalanced data, 2023.
- [58] Peter Sůkeník, Marco Mondelli, and Christoph H Lampert. Deep neural collapse is provably optimal for the deep unconstrained features model. *Advances in Neural Information Processing Systems*, 36, 2024.
- [59] Duc Anh Nguyen, Ron Levie, Julian Liene, Eyke Hüllermeier, and Gitta Kutyniok. Memorization-dilation: Modeling neural collapse under noise. In *The Eleventh International Conference on Learning Representations*, 2023.
- [60] Zhisheng Zhong, Jiequan Cui, Yibo Yang, Xiaoyang Wu, Xiaojuan Qi, Xiangyu Zhang, and Jiaya Jia. Understanding imbalanced semantic segmentation through neural collapse. In *Proceedings of the IEEE/CVF Conference on Computer Vision and Pattern Recognition*, pages 19550–19560, 2023.
- [61] Xuanton Liu, Jianfeng Zhang, Tianyang Hu, He Cao, Yuan Yao, and Lujia Pan. Inducing neural collapse in deep long-tailed learning. In *International Conference on Artificial Intelligence and Statistics*, pages 11534–11544. PMLR, 2023.
- [62] Peifeng Gao, Qianqian Xu, Peisong Wen, Huiyang Shao, Zhiyong Yang, and Qingming Huang. A study of neural collapse phenomenon: Grassmannian frame, symmetry and generalization, 2023.
- [63] Mufan Bill Li, Mihai Nica, and Daniel M. Roy. The neural covariance sde: Shaped infinite depth-and-width networks at initialization, 2023.
- [64] Zhanxuan Hu, Yichen Wang, Hailong Ning, Yonghang Tai, and Feiping Nie. Neural collapse inspired semi-supervised learning with fixed classifier. *Information Sciences*, 667:120469, 2024.
- [65] Gao Peifeng, Qianqian Xu, Yibo Yang, Peisong Wen, Huiyang Shao, Zhiyong Yang, Bernard Ghanem, and Qingming Huang. Towards demystifying the generalization behaviors when neural collapse emerges, 2024.
- [66] Alec Radford, Jeff Wu, Rewon Child, David Luan, Dario Amodei, and Ilya Sutskever. Language models are unsupervised multitask learners. 2019.
- [67] Nelson Elhage, Tristan Hume, Catherine Olsson, Nicholas Schiefer, Tom Henighan, Shauna Kravec, Zac Hatfield-Dodds, Robert Lasenby, Dawn Drain, Carol Chen, Roger Grosse, Sam McCandlish, Jared Kaplan, Dario Amodei, Martin Wattenberg, and Christopher Olah. Toy models of superposition. *Transformer Circuits Thread*, 2022. https://transformer-circuits.pub/2022/toy_model/index.html.
- [68] Christos Thrampoulidis, Ganesh Ramachandra Kini, Vala Vakilian, and Tina Behnia. Imbalance trouble: Revisiting neural-collapse geometry. *Advances in Neural Information Processing Systems*, 35:27225–27238, 2022.

- [69] Nagarajan Natarajan, Inderjit S Dhillon, Pradeep K Ravikumar, and Ambuj Tewari. Learning with noisy labels. *Advances in neural information processing systems*, 26, 2013.
- [70] Quinn Fisher, Haoming Meng, and Vardan Papyan. Pushing boundaries: Mixup’s influence on neural collapse, 2024.
- [71] Kaiming He, Xiangyu Zhang, Shaoqing Ren, and Jian Sun. Deep residual learning for image recognition. In *Proceedings of the IEEE conference on computer vision and pattern recognition*, pages 770–778, 2016.
- [72] David Mimno and Laure Thompson. The strange geometry of skip-gram with negative sampling. In Martha Palmer, Rebecca Hwa, and Sebastian Riedel, editors, *Proceedings of the 2017 Conference on Empirical Methods in Natural Language Processing*, pages 2873–2878, Copenhagen, Denmark, September 2017. Association for Computational Linguistics.
- [73] Kawin Ethayarajh. How contextual are contextualized word representations? comparing the geometry of bert, elmo, and gpt-2 embeddings, 2019.
- [74] Alex Wang, Amanpreet Singh, Julian Michael, Felix Hill, Omer Levy, and Samuel R. Bowman. Glue: A multi-task benchmark and analysis platform for natural language understanding, 2019.
- [75] Jia Hui Feng, Edmund M-K Lai, and Weihua Li. A study of neural collapse for text classification. In *International Conference on Deep Learning Theory and Applications*, pages 126–142. Springer, 2023.
- [76] Thomas Laurent, James H. von Brecht, and Xavier Bresson. Feature collapse, 2023.
- [77] Tom Brown, Benjamin Mann, Nick Ryder, Melanie Subbiah, Jared D Kaplan, Prafulla Dhariwal, Arvind Neelakantan, Pranav Shyam, Girish Sastry, Amanda Askell, et al. Language models are few-shot learners. *Advances in neural information processing systems*, 33:1877–1901, 2020.
- [78] Sid Black, Leo Gao, Phil Wang, Connor Leahy, and Stella Biderman. GPT-Neo: Large Scale Autoregressive Language Modeling with Mesh-Tensorflow, March 2021. If you use this software, please cite it using these metadata.
- [79] Susan Zhang, Stephen Roller, Naman Goyal, Mikel Artetxe, Moya Chen, Shuohui Chen, Christopher Dewan, Mona Diab, Xian Li, Xi Victoria Lin, Todor Mihaylov, Myle Ott, Sam Shleifer, Kurt Shuster, Daniel Simig, Punit Singh Koura, Anjali Sridhar, Tianlu Wang, and Luke Zettlemoyer. Opt: Open pre-trained transformer language models, 2022.
- [80] Hugo Touvron, Thibaut Lavril, Gautier Izacard, Xavier Martinet, Marie-Anne Lachaux, Timothée Lacroix, Baptiste Rozière, Naman Goyal, Eric Hambro, Faisal Azhar, Aurelien Rodriguez, Armand Joulin, Edouard Grave, and Guillaume Lample. Llama: Open and efficient foundation language models, 2023.
- [81] Albert Q. Jiang, Alexandre Sablayrolles, Arthur Mensch, Chris Bamford, Devendra Singh Chaplot, Diego de las Casas, Florian Bressand, Gianna Lengyel, Guillaume Lample, Lucile Saulnier, L  lio Renard Lavaud, Marie-Anne Lachaux, Pierre Stock, Teven Le Scao, Thibaut Lavril, Thomas Wang, Timoth  e Lacroix, and William El Sayed. Mistral 7b, 2023.
- [82] Ronald A Fisher. The use of multiple measurements in taxonomic problems. *Annals of eugenics*, 7(2):179–188, 1936.
- [83] C Radhakrishna Rao. The utilization of multiple measurements in problems of biological classification. *Journal of the Royal Statistical Society. Series B (Methodological)*, 10(2):159–203, 1948.
- [84] Thomas Strohmer and Robert W Heath Jr. Grassmannian frames with applications to coding and communication. *Applied and computational harmonic analysis*, 14(3):257–275, 2003.
- [85] Shayne FD Waldron. *An introduction to finite tight frames*. Springer, 2018.

- [86] David L Donoho, Michael Elad, and Vladimir N Temlyakov. Stable recovery of sparse overcomplete representations in the presence of noise. *IEEE Transactions on information theory*, 52(1):6–18, 2005.
- [87] Joel A Tropp. Just relax: Convex programming methods for identifying sparse signals in noise. *IEEE transactions on information theory*, 52(3):1030–1051, 2006.
- [88] Vardan Papayan. Traces of class/cross-class structure pervade deep learning spectra, 2020.
- [89] Christopher R. Hoyt and Art B. Owen. Probing neural networks with t-sne, class-specific projections and a guided tour, 2021.
- [90] John Zarka, Florentin Guth, and Stéphane Mallat. Separation and concentration in deep networks, 2021.
- [91] Tomer Galanti, Liane Galanti, and Ido Ben-Shaul. On the implicit bias towards minimal depth of deep neural networks, 2022.
- [92] Ido Ben-Shaul and Shai Dekel. Nearest class-center simplification through intermediate layers. In Alexander Cloninger, Timothy Doster, Tegan Emerson, Manohar Kaul, Ira Ktena, Henry Kvinge, Nina Miolane, Bastian Rieck, Sarah Tymochko, and Guy Wolf, editors, *Proceedings of Topological, Algebraic, and Geometric Learning Workshops 2022*, volume 196 of *Proceedings of Machine Learning Research*, pages 37–47. PMLR, 25 Feb–22 Jul 2022.
- [93] Hangfeng He and Weijie J. Su. A law of data separation in deep learning, 2022.
- [94] Liam Parker, Emre Onal, Anton Stengel, and Jake Intrater. Neural collapse in the intermediate hidden layers of classification neural networks, 2023.
- [95] Akshay Rangamani, Marius Lindegaard, Tomer Galanti, and Tomaso A Poggio. Feature learning in deep classifiers through intermediate neural collapse. In Andreas Krause, Emma Brunskill, Kyunghyun Cho, Barbara Engelhardt, Sivan Sabato, and Jonathan Scarlett, editors, *Proceedings of the 40th International Conference on Machine Learning*, volume 202 of *Proceedings of Machine Learning Research*, pages 28729–28745. PMLR, 23–29 Jul 2023.
- [96] Wojciech Masarczyk, Mateusz Ostaszewski, Ehsan Imani, Razvan Pascanu, Piotr Mił oś, and Tomasz Trzcinski. The tunnel effect: Building data representations in deep neural networks. In A. Oh, T. Naumann, A. Globerson, K. Saenko, M. Hardt, and S. Levine, editors, *Advances in Neural Information Processing Systems*, volume 36, pages 76772–76805. Curran Associates, Inc., 2023.
- [97] Daniel Beaglehole, Peter Súkeník, Marco Mondelli, and Mikhail Belkin. Average gradient outer product as a mechanism for deep neural collapse, 2024.
- [98] Peng Wang, Xiao Li, Can Yaras, Zhihui Zhu, Laura Balzano, Wei Hu, and Qing Qu. Understanding deep representation learning via layerwise feature compression and discrimination, 2024.
- [99] Sicong Wang, Kuo Gai, and Shihua Zhang. Progressive feedforward collapse of resnet training, 2024.
- [100] Connall Garrod and Jonathan P. Keating. Unifying low dimensional observations in deep learning through the deep linear unconstrained feature model, 2024.
- [101] Emanuele Zangrando, Piero Deidda, Simone Brugiapaglia, Nicola Guglielmi, and Francesco Tudisco. Neural rank collapse: Weight decay and small within-class variability yield low-rank bias, 2024.
- [102] Mengjia Xu, Akshay Rangamani, Qianli Liao, Tomer Galanti, and Tomaso Poggio. Dynamics in deep classifiers trained with the square loss: Normalization, low rank, neural collapse, and generalization bounds. *Research*, 6:0024, 2023.
- [103] Tong Liang and Jim Davis. Inducing neural collapse to a fixed hierarchy-aware frame for reducing mistake severity. In *Proceedings of the IEEE/CVF International Conference on Computer Vision*, pages 1443–1452, 2023.

- [104] Guglielmo Bonifazi, Iason Chalas, Gian Hess, and Jakub Łucki. Can we understand plasticity through neural collapse?, 2024.
- [105] Ilya Sutskever, Aug 2023.
- [106] Li Guo, Keith Ross, Zifan Zhao, George Andriopoulos, Shuyang Ling, Yufeng Xu, and Zixuan Dong. Cross entropy versus label smoothing: A neural collapse perspective, 2024.
- [107] Neil Burgess, Jelena Milanovic, Nigel Stephens, Konstantinos Monachopoulos, and David Mansell. Bfloat16 processing for neural networks. In *2019 IEEE 26th Symposium on Computer Arithmetic (ARITH)*, pages 88–91, 2019.

A Architectural Details

Table 2: Sample architectural configuration for a 12-layer 1024-dimensional causal language model (CLM) based on [2] and GPT-Neo [78]. Shallower models have configurations with `attention_layers` and `attention_types` truncated. Narrower models adjust `hidden_size` to their width (d). All other configuration values are the same across models.

SETTING	VALUE
<code>activation_function</code>	<code>gelu_new</code>
<code>architectures</code>	<code>GPTNeoForCausalLM</code>
<code>attention_dropout</code>	<code>0</code>
<code>attention_layers</code>	<code>global, local, global, local, ...</code>
<code>attention_types</code>	<code>[[global, local], 6]</code>
<code>bos_token_id</code>	<code>50256</code>
<code>embed_dropout</code>	<code>0</code>
<code>eos_token_id</code>	<code>50256</code>
<code>gradient_checkpointing</code>	<code>false</code>
<code>hidden_size</code>	<code>1024</code>
<code>initializer_range</code>	<code>0.02</code>
<code>intermediate_size</code>	<code>null</code>
<code>layer_norm_epsilon</code>	<code>1e-05</code>
<code>max_position_embeddings</code>	<code>2048</code>
<code>model_type</code>	<code>gpt_neo</code>
<code>num_heads</code>	<code>16</code>
<code>num_layers</code>	<code>12</code>
<code>resid_dropout</code>	<code>0</code>
<code>summary_activation</code>	<code>null</code>
<code>summary_first_dropout</code>	<code>0.1</code>
<code>summary_proj_to_labels</code>	<code>true</code>
<code>summary_type</code>	<code>cls_index</code>
<code>summary_use_proj</code>	<code>true</code>
<code>torch_dtype</code>	<code>float32</code>
<code>transformers_version</code>	<code>4.28.1</code>
<code>use_cache</code>	<code>true</code>
<code>vocab_size</code>	<code>50257</code>
<code>window_size</code>	<code>256</code>

B Dataset

TinyStories is a synthetic dataset of short children’s stories generated by GPT-3.5 and GPT-4 [2].

- The dataset is released with the CDLA-Sharing-1.0 licence.
- Our models were trained and evaluated using the first version of TinyStories [2].
- The 2,141,709 stories are split into 2,119,719 train and 21,990 validation stories.
- Their experimental setup [2] called for the GPT-2 [66] tokenizer, of which only a subset vocabulary \mathcal{V} of size 29,233 appears in TinyStories.
- Following the GPT-style regime for training/evaluation [5], raw sequences (stories) from the train set are packed into 229,367 (S) chunks of 2048 (T) tokens each. This setup provides 469,514,249 (N) ground-truth¹⁶ token samples for training.
- Dataloading and preprocessing (including chunking) each used two workers.

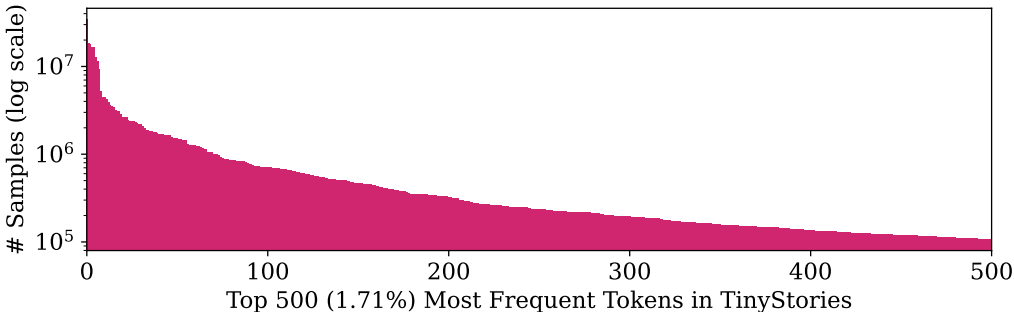


Figure 4: The 500 most frequent classes from TinyStories [2] exhibit significant sample imbalance.

C Optimization

Training was performed using an adaptation of an open-source causal language modeling script from Huggingface: https://github.com/huggingface/transformers/blob/main/examples/pytorch/language-modeling/run_clm.py

- Each model was trained on a single NVIDIA A100 (40GB) GPU for up to 8 hours per epoch.
- Learning rates were set by a linear schedule based on the number of steps with no warm-up.
- Training was performed in bfloat16 [107] mixed precision.
- The results presented in this work are from two sets of models trained with weight decay $\beta = 0.0005$ [50] and $\beta = 0.1$ [77]. A previous set of models was trained without weight decay and the results are very similar to $\beta = 0.0005$.

Table 3: Batch sizes used to train models on a single NVIDIA A100 (40GB) GPU. Width (d) and depth (L) correspond to hidden_size and length of attention_layers, respectively, in Table 2.

DEPTH (L) ↓	WIDTH (d) →	64	128	256	512	768	1024
1-layer		16	16	16	16	16	16
2-layer		16	16	16	16	16	8
4-layer		8	8	8	8	8	8
8-layer		8	8	8	4	4	4
12-layer		4	4	4	4	4	4

¹⁶ $N = S(T - 1)$ as we cannot use the first ground-truth nor the last predicted token in any chunk.

D Within-Class Variability Collapse with Scale – $\mathcal{NC1}$

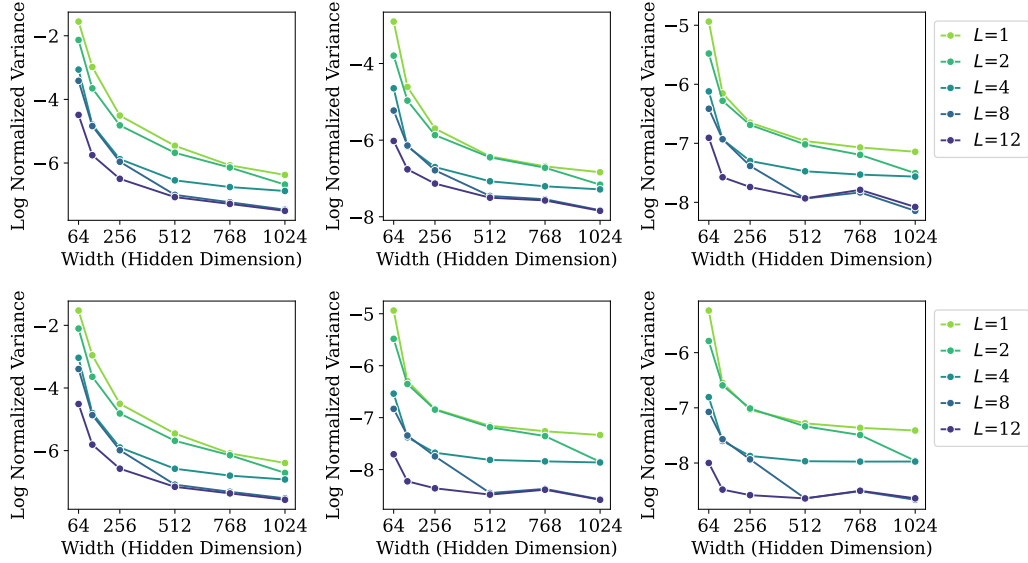


Figure 5: Average (logarithmic) class-distance normalized variance (CDNV) is reduced ($\mathcal{NC1}$) when scaling width (d) and across training for 1 (left) through 10 (right) epochs with weight decays $\beta = 0.0005$ (top) and $\beta = 0.1$ (bottom).

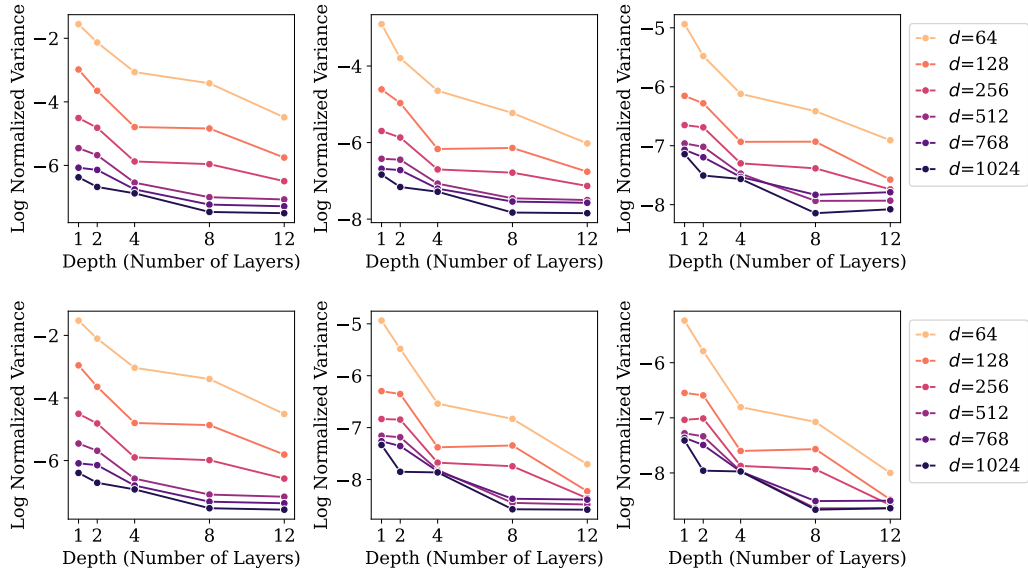


Figure 6: Average (logarithmic) class-distance normalized variance (CDNV) is reduced ($\mathcal{NC1}$) when scaling depth (L) and across training for 1 (left) through 10 (right) epochs with weight decays $\beta = 0.0005$ (top) and $\beta = 0.1$ (bottom).

E Mean Norms Growth with Scale – (Related to $\mathcal{N}C2$)

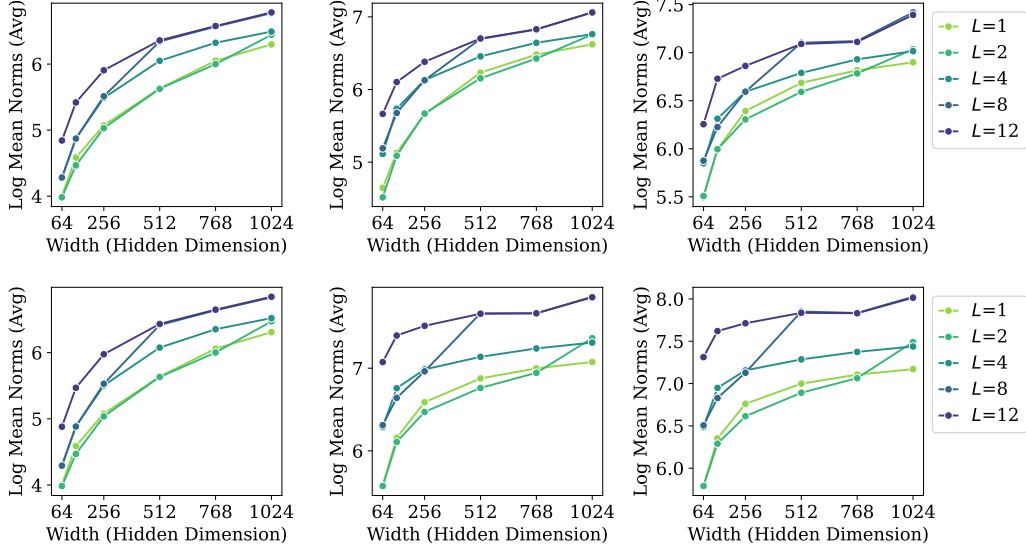


Figure 7: Class embedding mean norms grow when scaling width (d) and across training for 1 (left) through 10 (right) epochs with weight decays $\beta = 0.0005$ (top) and $\beta = 0.1$ (bottom).

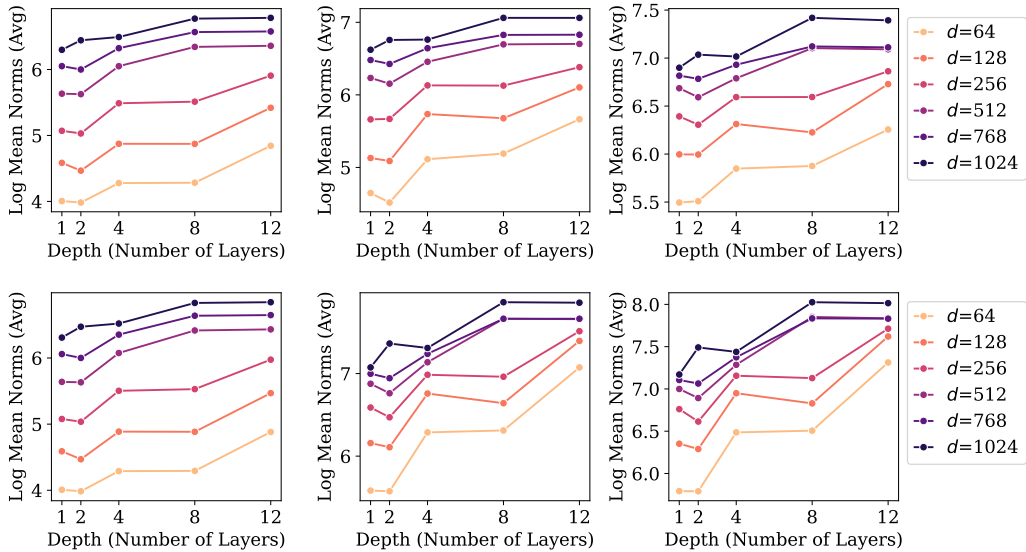


Figure 8: Class embedding mean norms grow when scaling depth (L) and across training for 1 (left) through 10 (right) epochs with weight decays $\beta = 0.0005$ (top) and $\beta = 0.1$ (bottom).

F Equinormness with Scale – $\mathcal{NC}2$

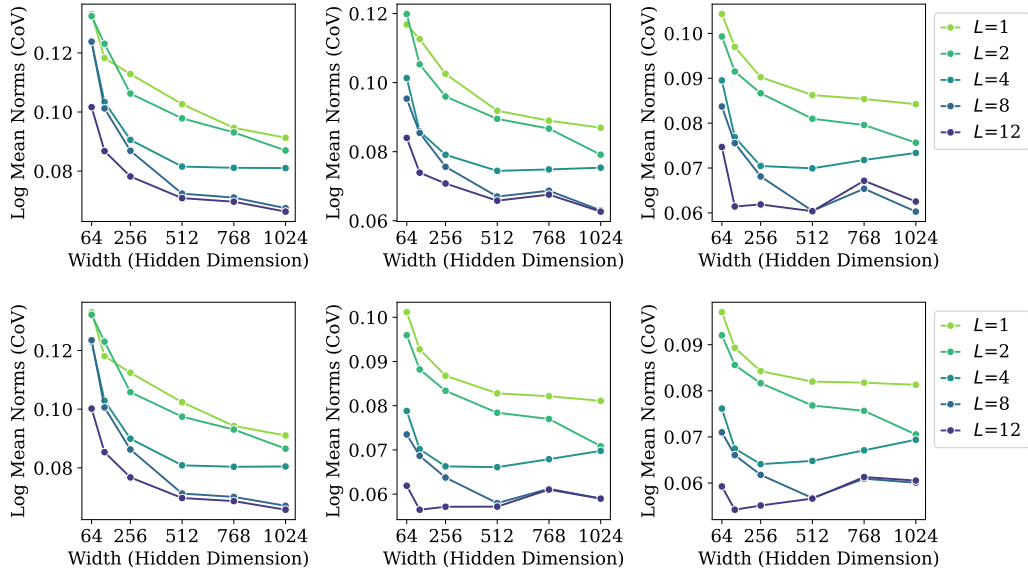


Figure 9: Variation in embedding norms decreases ($\mathcal{NC}2$) when scaling width (d) in models trained for 1 (left) through 10 (right) with weight decays $\beta = 0.0005$ (top) and $\beta = 0.1$ (bottom). Note that the degree of equinormness eventually plateaus for sufficiently deep and trained models.

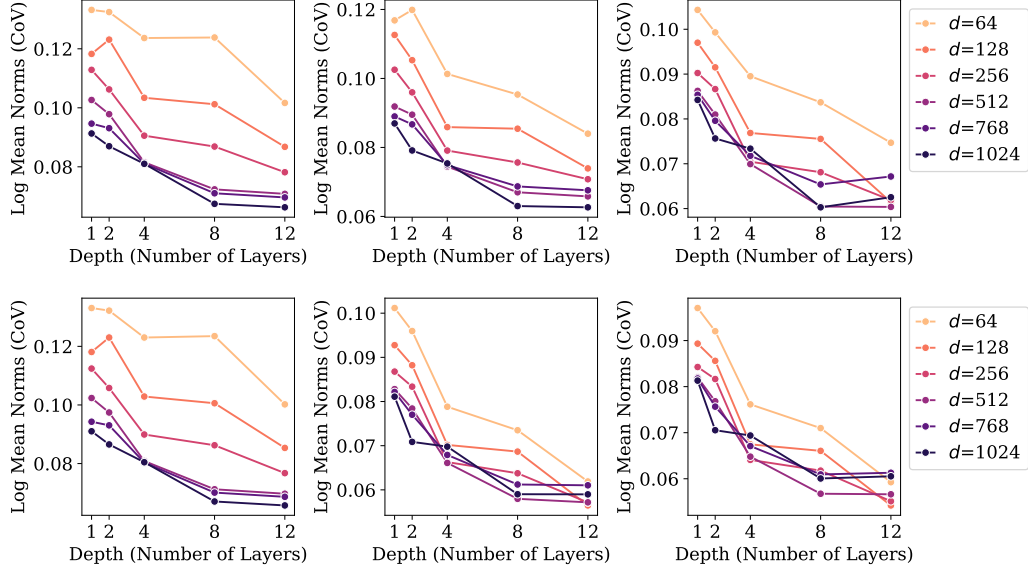


Figure 10: Variation in embedding norms decreases ($\mathcal{NC}2$) when scaling depth (L) in models trained for 1 (left) through 10 (right) with weight decays $\beta = 0.0005$ (top) and $\beta = 0.1$ (bottom).

G Interference with Scale – (Related to $\mathcal{NC}2$)

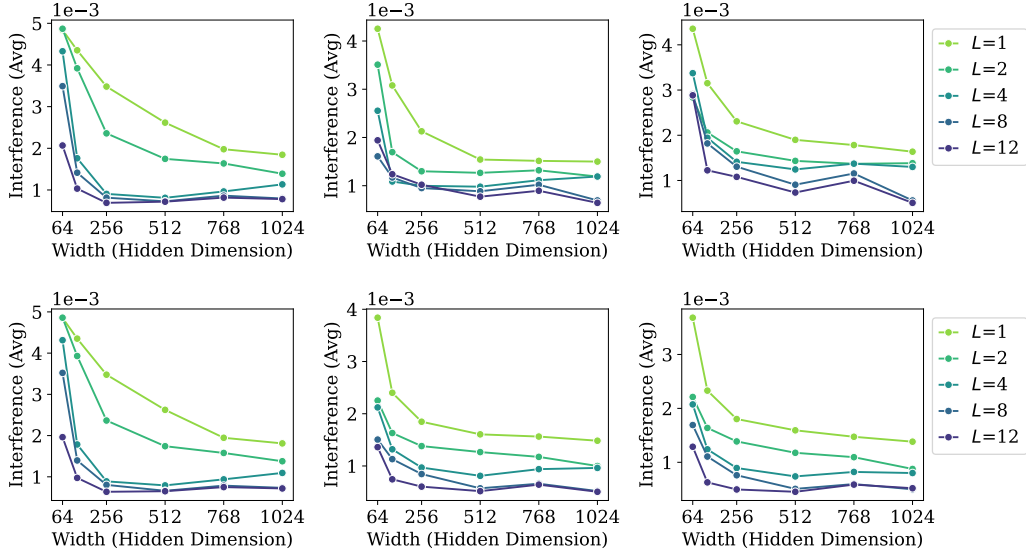


Figure 11: Average interference decreases (to some extent) when scaling width (d) in models trained for 1 (left) through 10 (right) with weight decays $\beta = 0.0005$ (top) and $\beta = 0.1$ (bottom).

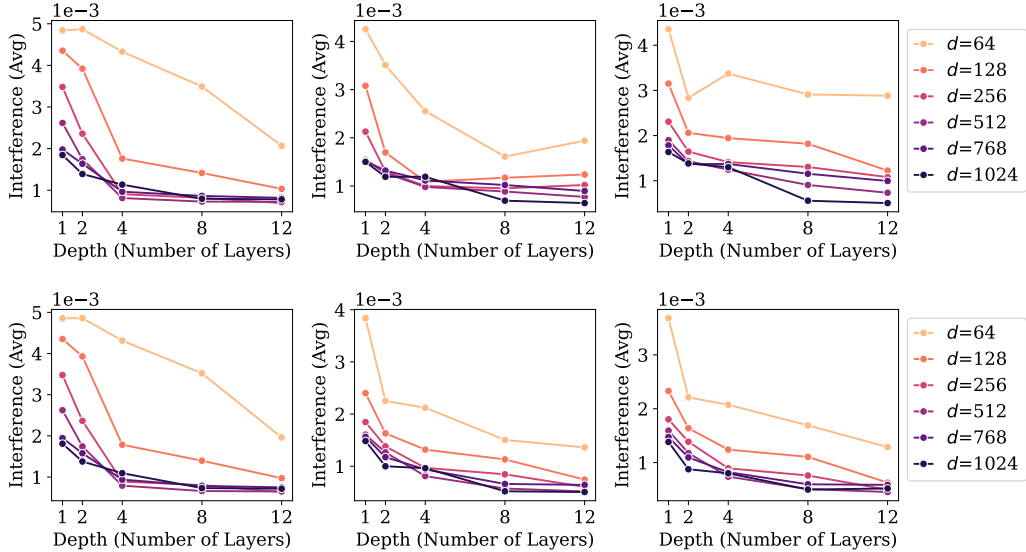


Figure 12: Average interference decreases (to some extent) when scaling depth (L) in models trained for 1 (left) through 10 (right) with weight decays $\beta = 0.0005$ (top) and $\beta = 0.1$ (bottom).

H Equiangularity with Scale – (Against $\mathcal{NC}2$)

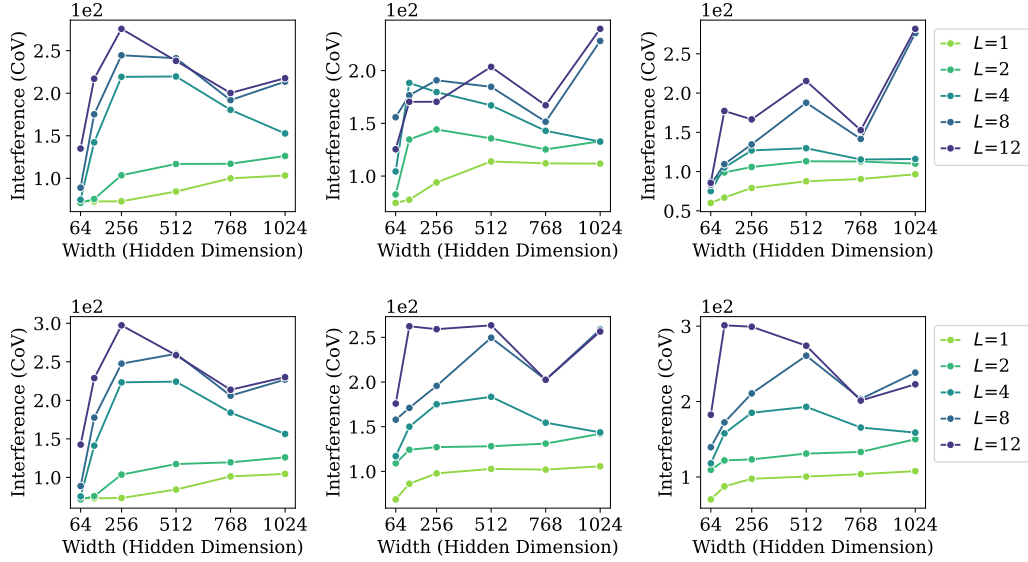


Figure 13: Variation in interference roughly increases when scaling width (d) in models trained for 1 (left) through 10 (right) with weight decays $\beta = 0.0005$ (top) and $\beta = 0.1$ (bottom). Note this trend is against equiangularity, affirming the traditional $\mathcal{NC}2$ to be less useful than $\mathcal{GN}C2$ [16].

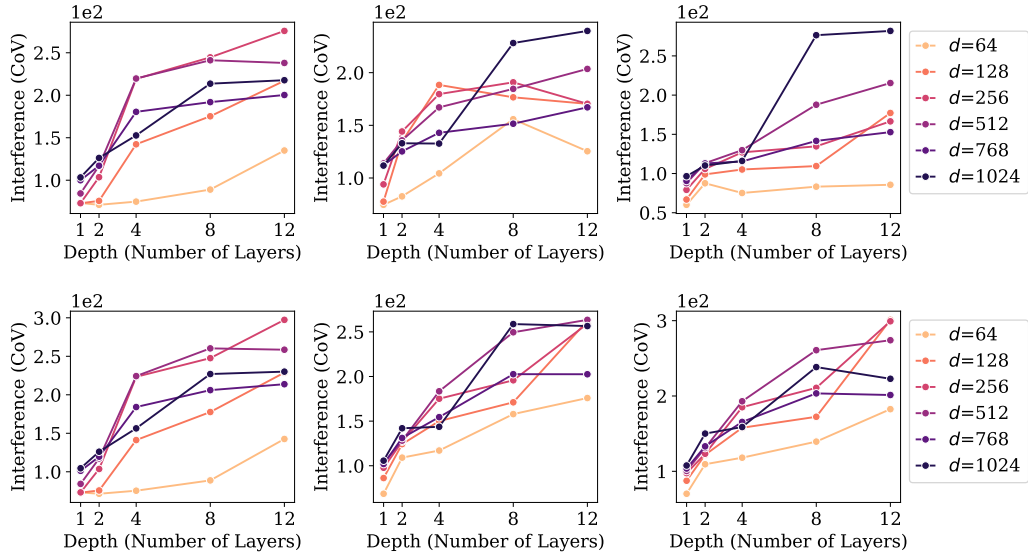


Figure 14: Variation in interference increases when scaling depth (L) in models trained for 1 (left) through 10 (right) with weight decays $\beta = 0.0005$ (top) and $\beta = 0.1$ (bottom). Note this trend is against equiangularity, affirming the traditional $\mathcal{NC}2$ to be less useful than $\mathcal{GN}C2$ [16].

I Logarithmic Distances with Scale – (Related to $\mathcal{GN}C2$)

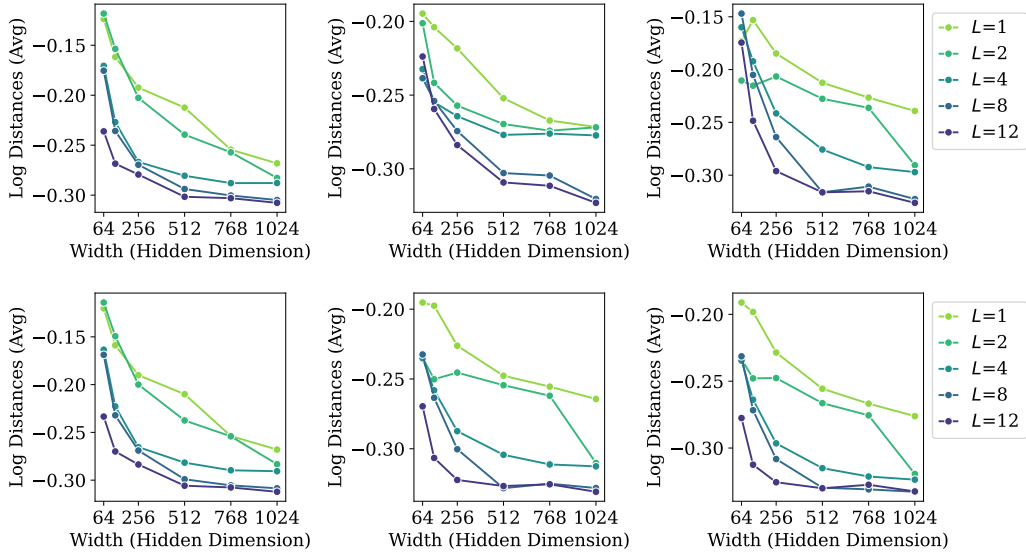


Figure 15: Average logarithmic distance decreases when scaling width (d) in models trained for 1 (left) through 10 (right) with weight decays $\beta = 0.0005$ (top) and $\beta = 0.1$ (bottom).

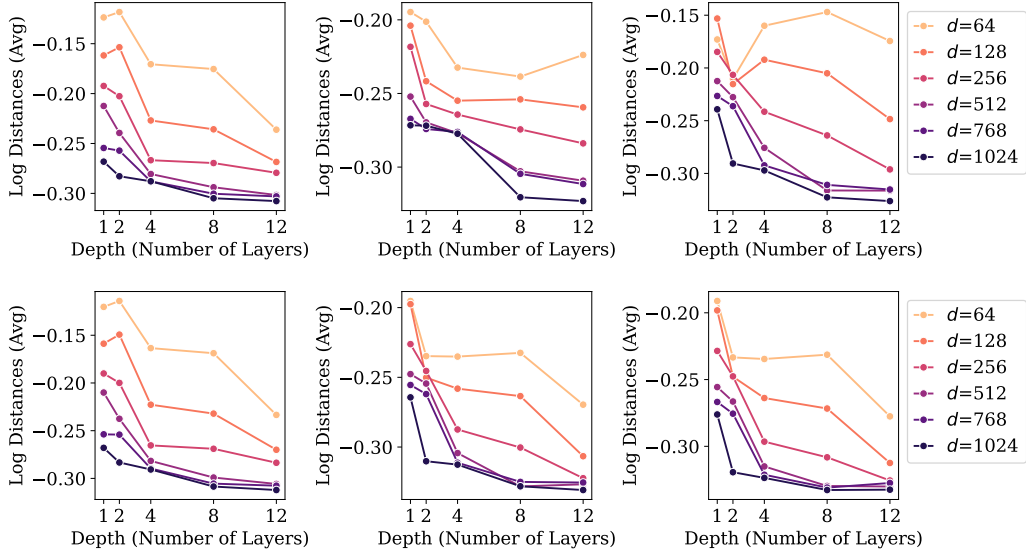


Figure 16: Average logarithmic distance decreases when scaling depth (L) in models trained for 1 (left) through 10 (right) with weight decays $\beta = 0.0005$ (top) and $\beta = 0.1$ (bottom).

J Hyperspherical Uniformity with Scale – $\mathcal{GN}C2$

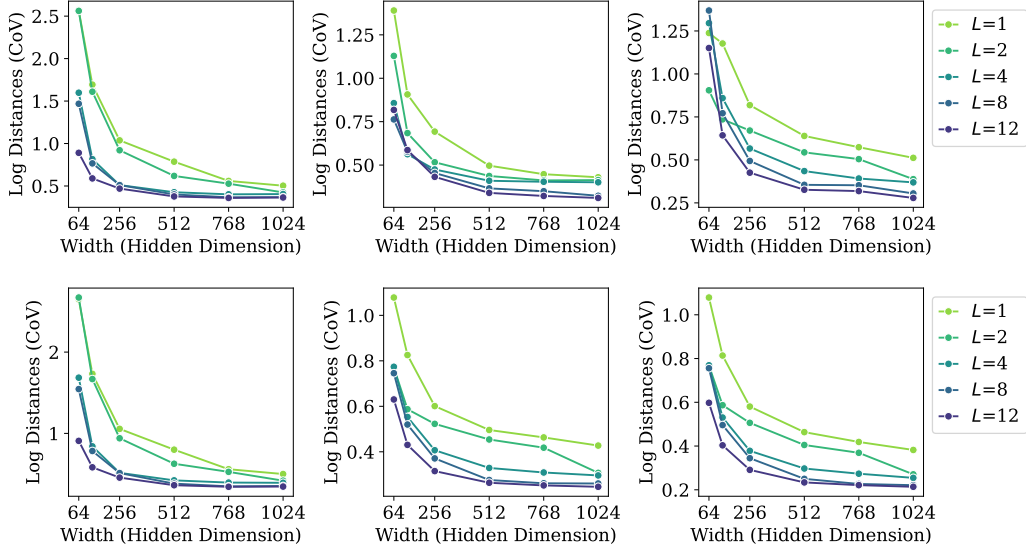


Figure 17: Variation in logarithmic distances decreases when scaling width (d) in models trained for 1 (left) through 10 (right) with weight decays $\beta = 0.0005$ (top) and $\beta = 0.1$ (bottom). This consistent trend towards hyperspherical uniformity affirms that $\mathcal{GN}C2$ [16] is more useful than $\mathcal{NC}2$.

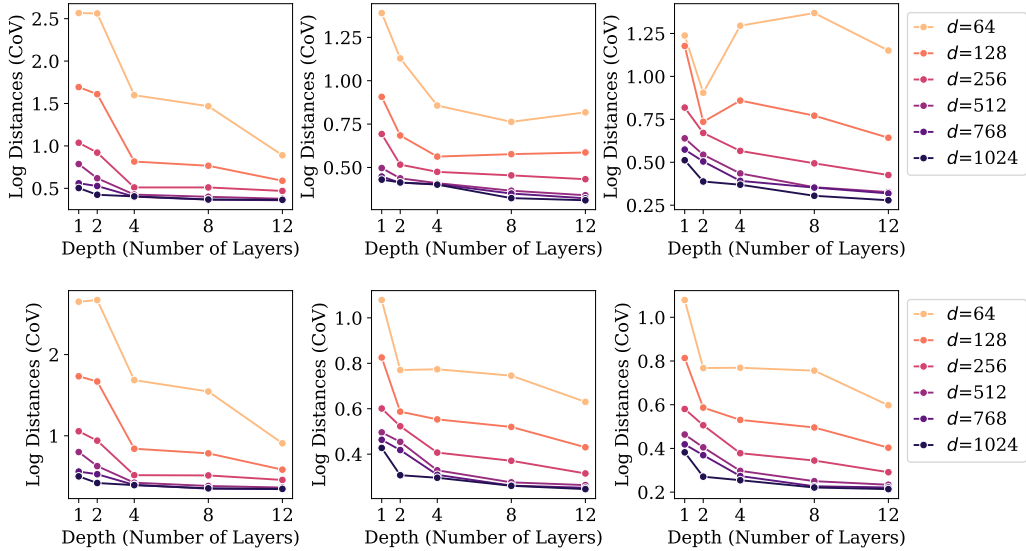


Figure 18: Variation in logarithmic distances decreases when scaling depth (L) in models trained for 1 (left) through 10 (right) with weight decays $\beta = 0.0005$ (top) and $\beta = 0.1$ (bottom). This consistent trend towards hyperspherical uniformity affirms that $\mathcal{GN}C2$ [16] is more useful than $\mathcal{NC}2$.

K Self-Duality with Scale – (Against $\mathcal{NC3}$)

Self-duality ($\mathcal{NC3}$) was originally the convergence of classifiers to class means after normalization:

$$\left\| \frac{\mathbf{w}_c}{\|\mathbf{w}_c\|_2} - \frac{\boldsymbol{\mu}_c - \bar{\boldsymbol{\mu}}}{\|\boldsymbol{\mu}_c - \bar{\boldsymbol{\mu}}\|_2} \right\|_2 \rightarrow 0, \quad \forall c. \quad (11)$$

Instead, we use class-wise similarity (Equation 8) and its variation ($\mathcal{UNC3}$).

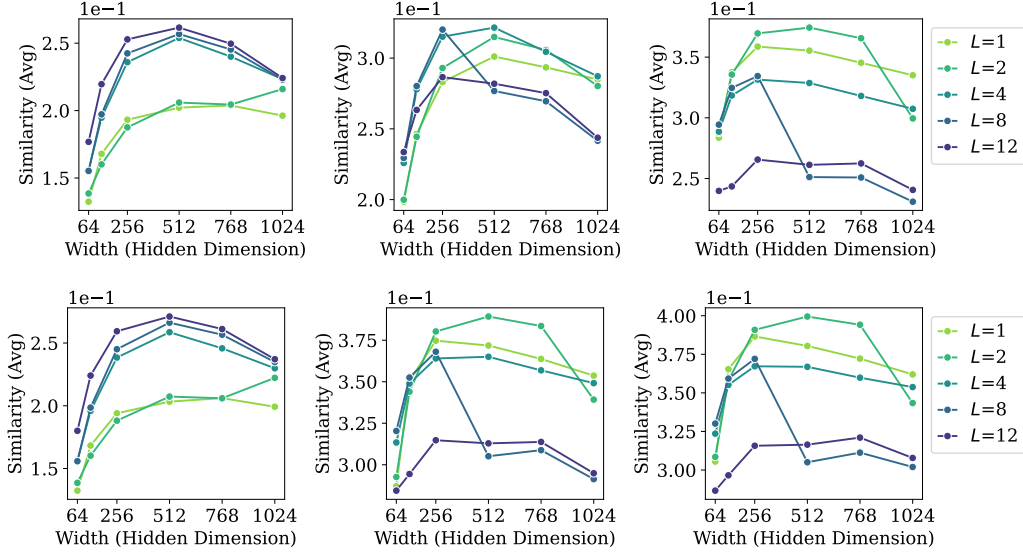


Figure 19: Average classifier alignment increases $\mathcal{NC3}$ when training for 1 (left) through 10 (right) with weight decays $\beta = 0.0005$ (top) and $\beta = 0.1$ (bottom). However, we see no meaningful trend when scaling width d , suggesting that $\mathcal{NC3}$ does not coalesce with language modeling training.

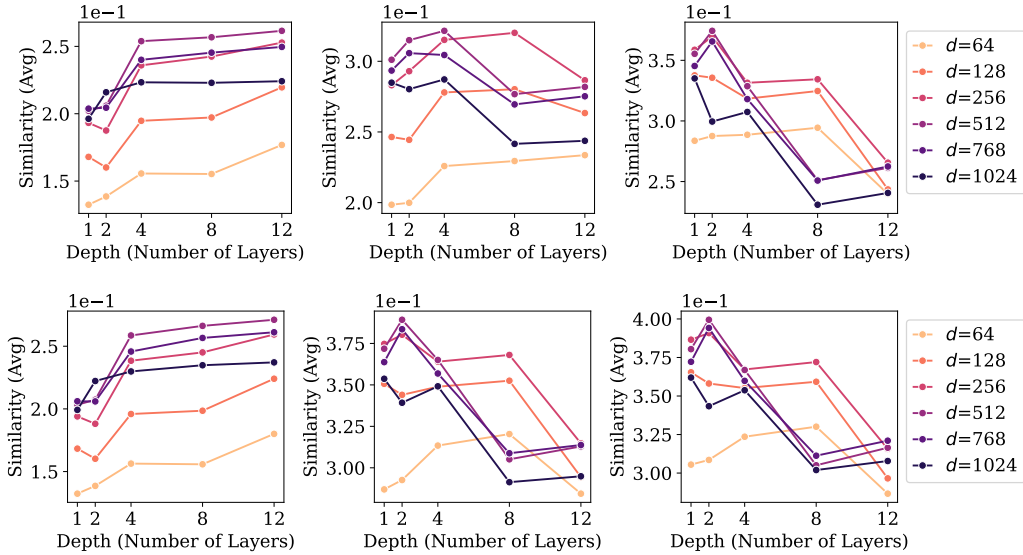


Figure 20: Average classifier alignment increases $\mathcal{NC3}$ when training for 1 (left) through 10 (right) with weight decays $\beta = 0.0005$ (top) and $\beta = 0.1$ (bottom). However, we see no meaningful trend when scaling depth L , suggesting that $\mathcal{NC3}$ does not coalesce with language modeling training.

L Uniformity Duality with Scale – $\mathcal{UNC3}$

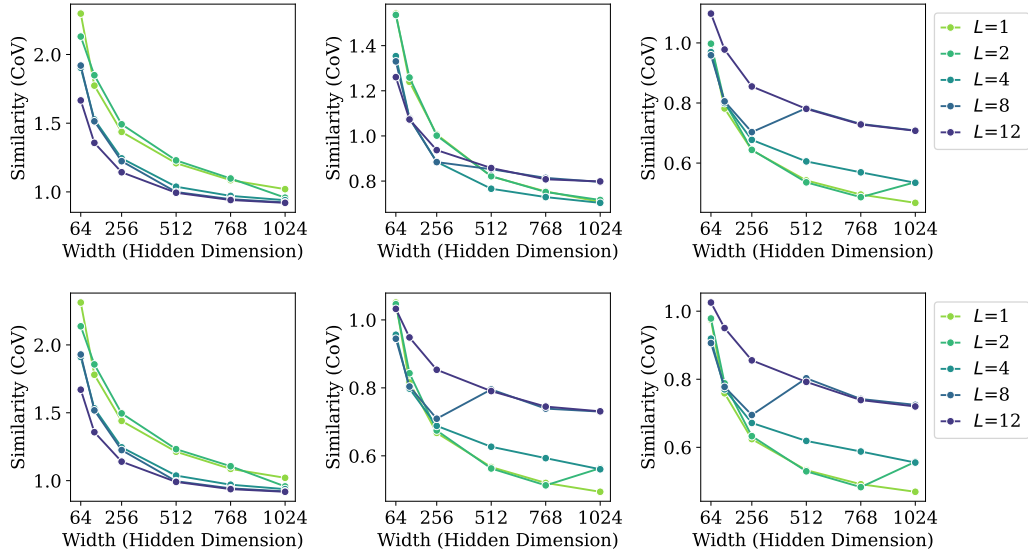


Figure 21: Variation in classifier alignment decreases when scaling width (d) in models trained for 1 (left) through 10 (right) with weight decays $\beta = 0.0005$ (top) and $\beta = 0.1$ (bottom).

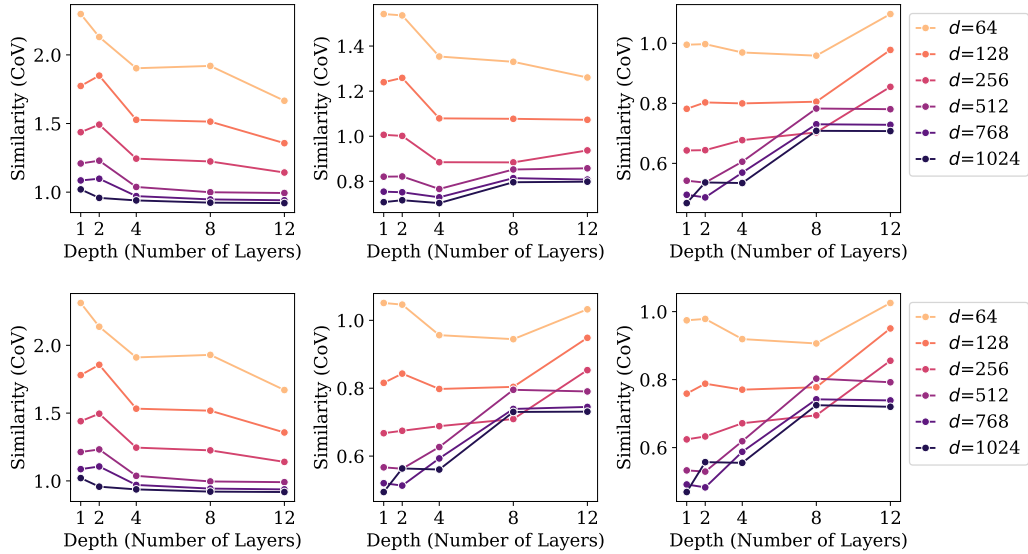


Figure 22: Variation in classifier alignment increases when scaling depth (L) in models trained for 1 (left) through 10 (right) with weight decays $\beta = 0.0005$ (top) and $\beta = 0.1$ (bottom). This negative trend of $\mathcal{UNC3}$ in more learnt models (right) suggests that the link of $(\mathcal{U})\mathcal{NC3}$ with scale and performance is still weak.

M Classifier Agreement – $\mathcal{NC4}$

For computational reasons, we compute Equations 9, 10 using a simple decomposition:

$$\operatorname{argmin}_{c \in \mathbb{V}} \|\mathbf{h}_b - \boldsymbol{\mu}_c\|_2 = \operatorname{argmin}_{c \in \mathbb{V}} \left(\|\mathbf{h}_b\|^2 + \|\boldsymbol{\mu}_c\|^2 - 2\mathbf{h}_b^\top \boldsymbol{\mu}_c \right) \quad (12)$$

where $b \in [1, B]$ and $c \in \mathbb{V}$ with batch size B and vocabulary \mathbb{V} .

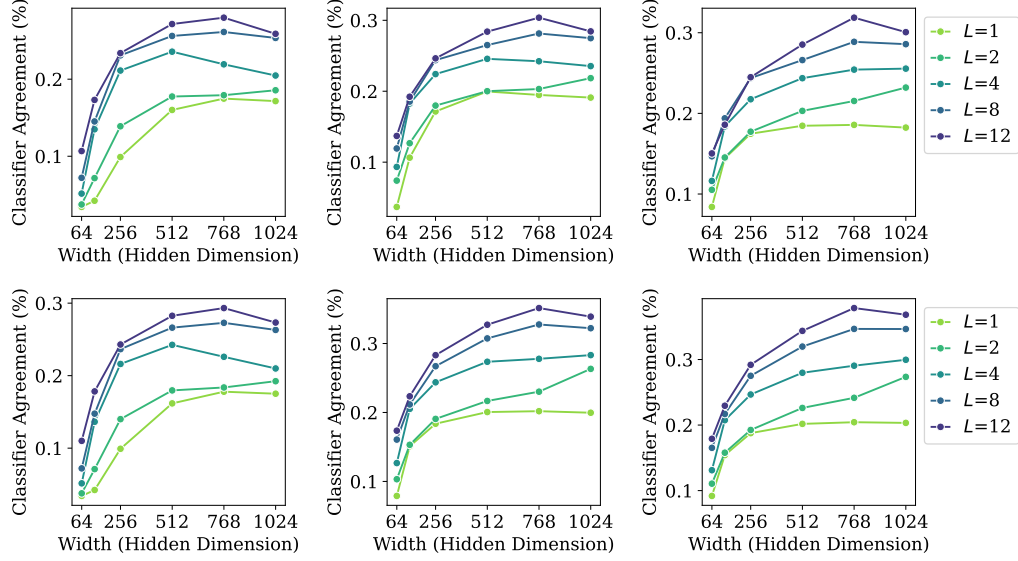


Figure 23: Classifier agreement improves when scaling width (d) in models trained for 1 (left) through 10 (right) with weight decays $\beta = 0.0005$ (top) and $\beta = 0.1$ (bottom).

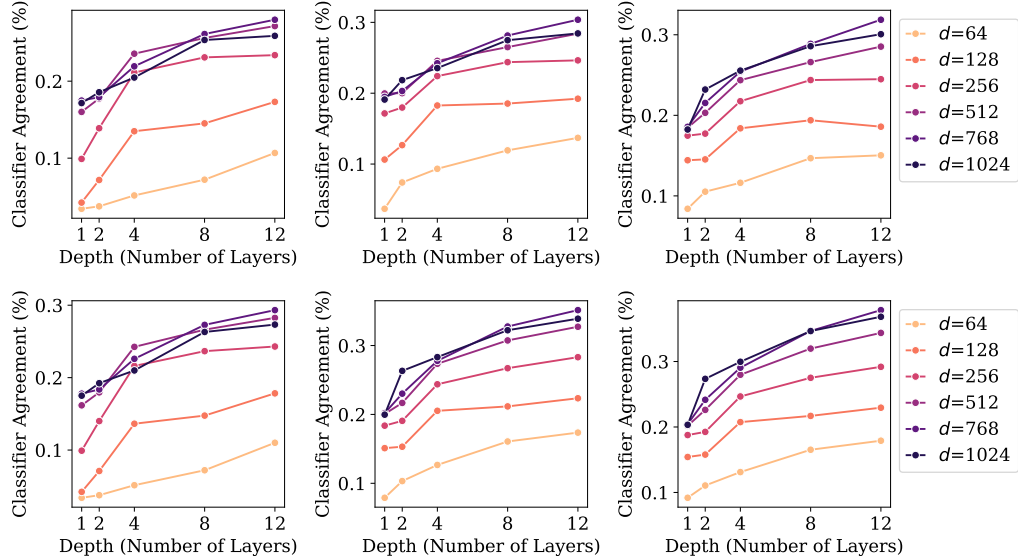


Figure 24: Classifier agreement improves when scaling depth (L) in models trained for 1 (left) through 10 (right) with weight decays $\beta = 0.0005$ (top) and $\beta = 0.1$ (bottom).

N Correlations with Generalization Performance

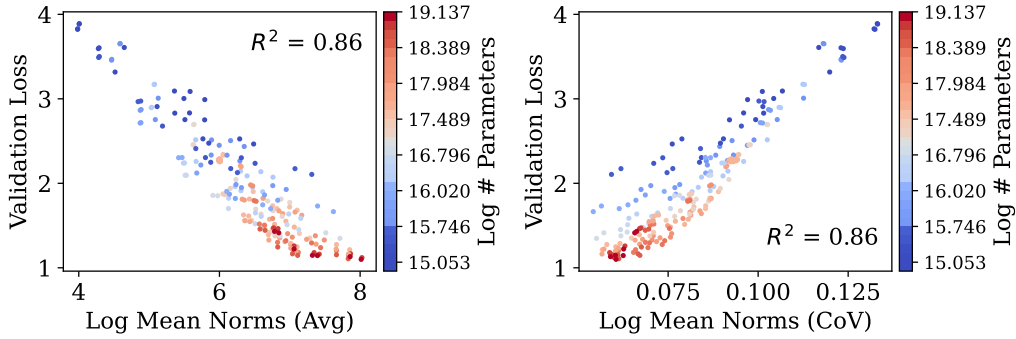


Figure 25: Validation loss shows some correlation with average mean norms (left) and their variations (\mathcal{NC}_2) (right).

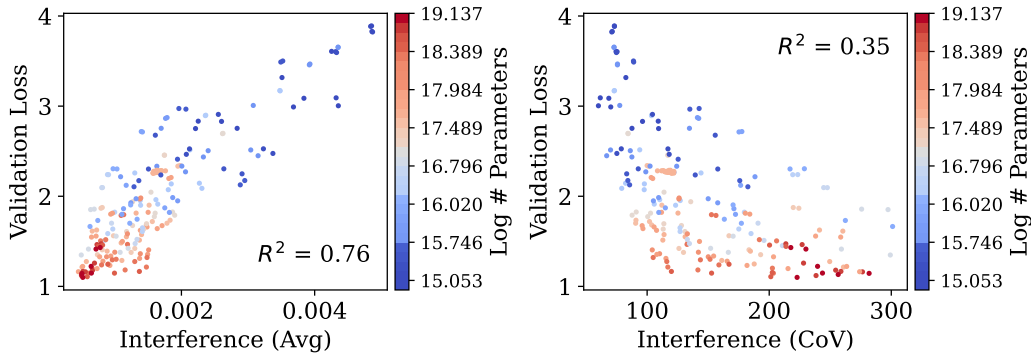


Figure 26: Validation loss shows weak correlation with average interference and almost none with its variation (i.e. equiangularity, \mathcal{NC}_2) (right).

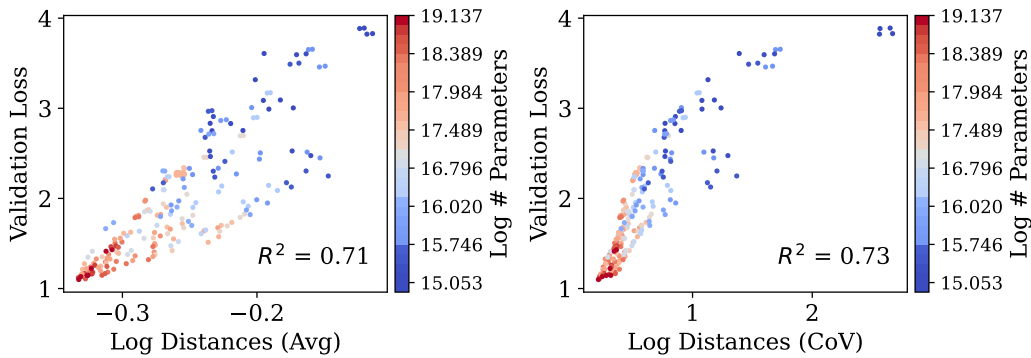


Figure 27: Validation loss shows some correlation with average kernel distances and with its variation (i.e. hyperspherical uniformity, \mathcal{GN}_2) (right).